Monitoring and Predicting Eutrophication of Inland Waters Using Remote Sensing

Shabani Marijani Mssanzya
February, 2010

Monitoring and Predicting Eutrophication of Inland Waters Using Remote Sensing

by

Shabani Marijani Mssanzya

Thesis submitted to the International Institute for Geo-information Science and Earth Observation in partial fulfilment of the requirements for the degree of Master of Science in Geo-information Science and Earth Observation, Specialisation: Environmental Hydrology

Thesis Assessment Board

Chairman:	Prof. Dr. Ing. Wouter Verhoef (ITC)
External Examiner:	Dr. M. A. Eleveld (Free University- Amsterdam)
First Supervisor:	Dr. Ir. Mhd. Suhyb Salama (ITC)
Second Supervisor:	Dr. Ir. Chris M. Mannaerts (ITC)
Advisor:	Ms. Wiwin Ambarwulan (ITC)

ITC

INTERNATIONAL INSTITUTE FOR GEO-INFORMATION SCIENCE AND EARTH OBSERVATION
ENSCHEDE, THE NETHERLANDS

Abstract

Inland waters are human kind assets as they serve for both economical and ecological well being; however, their existence is compromised by raising eutrophication in these water bodies' especially toxic cyanobacteria species. Existing in-situ water quality measurements have failed to offer required temporal and spatial coverage which cope with the dynamics of water quality. Therefore, the purpose of this thesis was to use remote sensing techniques to monitor and predict eutrophication with the focus on separating cyanobacteria from other Phytoplankton species.

Eutrophication in water bodies is associated with growth of Phytoplankton biomass which is easily to be detected by satellite sensors. Moreover; as eutrophication process is taking place, Inherent Optical Properties (IOP) of water changes accordingly. It is these IOPs which can be related to their respective concentration using bio optical models. From observation of the water leaving reflectance, we can determine the IOPs of different water constituents, namely: chlorophyll a, dissolved organic matter, particulate matters and cyanobacteria. The differences in spectral characteristics of water constituents make it possible to quantify them separately using remote sensing techniques.

In this thesis, GSM01 (Garver- Siegel- Maritorena) model was modified by removing band six of MERIS (centered at 620 nm) to exclude Phycocyanin pigments from derived Chlorophyll a concentration. This separation was possible because a Cyanobacterium which is determined by Phycocyanin pigments has maximum absorption at 620 nm. A simple analytical model was derived to retrieve absorption coefficients due to Phycocyanin pigments separately at 620. The method was validated using in-situ water quality measurements from Poyang Lake in China. The model gave good results on the relationships between derived absorption coefficients due to Phycocyanin pigments (a_{pc}) and Chlorophyll a concentration ($R^2 = 0.9$) which clearly prove the fact that at a certain concentration of chlorophyll a concentration (6.0 mg/$m^3$to around 15 mg/m^3according to the data set used) the relationship is strongly linear. Using derived products it was possible to develop Remote Sensed Eutrophication Indices (R.S.E.I.) by applying Principal Component analysis (PCA) which gave insight of having R.S.E.I which can replace in-situ derived indices.

Proposed model gave a promising approach to separate Chl-a and a_{pc} as well as developing R.S.E.I. which can surrogate in-situ derived E.I. and be used as a tool for monitoring and predicting eutrophication in inland waters. However, model overestimated chlorophyll a concentration which needs adjustments using more in-situ measurements, and derived R.S.E.I. and a_{pc} need validation using more in-situ data. Finally it was found that is not feasible to use remote sensing techniques for water quality management in small water bodies.

Acknowledgements

This thesis would not have been possible without the sponsorship of my studies in ITC by European Union via Erasmus mundus lot 10. With this sponsorship it has been possible for me to accomplish my studies with this thesis.

I am heartily thankful to my first supervisor Dr. Suhyb Salama for his tireless constructive critics and advices, he gave me courage and strength to accomplish my thesis, from him i learn more than remote sensing and water quality, i have learn to be critic to my own and others works and, i have learn to be positive and always find a solution in every problem, thank you Dr. Suhyb.

I extend my grateful thanks to my second supervisor Dr. Chris Mannaerts, I was lucky to have this water quality *guru* as my second supervisor, he brightly advised and commented on my work and made it possible to reach this stage, thank you Dr. Chris.

Many thanks also to my advisor Ms. Wiwim Ambarwulan, she has been there always whenever i needed her assistance, and to all my classmates who we have been together through out these challenging and tough times.

My deepest gratitude to my wife Simlizy for her distance support and courage, patience and understanding, she made me stronger and focused; she has been my comfort and a reason to keep moving on and reach this point.

Finally, I would like to thank my entire family, Tanzanian colleague, and whoever in a wide range of spectrum helped me anyhow and I didn’t mentioned, thank you all.

Thank God for sailing me through to this point.

Table of contents

List of figures

List of tables

List of Acronyms

CDOM	Coloured Dissolved Organic Matter
Chl-a	Chlorophyll a
DO	Dissolved oxygen
E. I	Eutrophication Index
ESA	European Space Agency
FR	Full Resolution
GSM	Garver-Siegel-Moritorena
IOP	Inherent Optical Properties
IR	Infra Red
MERIS	Medium Resolution Imaging Spectrometer
PC	Phycocyanin
PCA	Principal Component Analysis
RR	Reduced Resolution
RS	Remote Sensing
RS E.I	Remote Sensing Eutrophication Index
SIOP	Specific Inherent Optical Property
SPM	Suspended Particulate Matters
WFD	Water Framework Directive
WQ	Water Quality
WQI	Water Quality Index

List of Symbols used

Symbols	Description	Units
$a(\lambda)$	Bulk absorption coefficient	m^{-1}
$a^*(\lambda)$	Specific absorption coefficient	$m^2. mg^{-1}$
$a_{dg}(\lambda)$	Absorption coefficient of dissolved organic matter	m^{-1}
$a^*_{pc}(\lambda)$	Specific absorption coefficient of Phycocyanin	$m^2. mg^{-1}$
$a_{pc}(\lambda)$	Absorption coefficient of Phycocyanin	m^{-1}
$a_{Chl}(\lambda)$	Absorption coefficient of Chlorophyll a	m^{-1}
$a_w(\lambda)$	Absorption coefficient of water molecule	m^{-1}
$b(\lambda)$	Bulk scattering coefficient	m^{-1}
$b^*(\lambda)$	Specific scattering coefficient	$m^2. g^{-1}$
$b_b(\lambda)$	Bulk backward scattering coefficient	m^{-1}
$b_{bspm}(\lambda)$	Backward scattering coefficient of suspended particulate matters	m^{-1}
$b_{bw}(\lambda)$	Backward scattering coefficient of water molecules	m^{-1}
$R(0^-, \lambda)$	Subsurface irradiance reflectance	%
R_{rs}	Remote sensing reflectance	Sr^{-1}
α	Backscattering fraction	Dimensionless
S	Spectral exponent	Dimensionless
η	Power law exponent for particulate backscattering coefficient	Dimensionless
λ	Wavelength	m^{-1}
y	Spectral shape parameter	Dimensionless
t	Water- air transmission factor	Dimensionless
n_w	Index of refraction of the water	Dimensionless
g_i	Geometrical factor	Dimensionless

1. Introduction

Eutrophication is a major water quality problem worldwide, causing turbid water with high algal biomass and offering poor condition to the aquatic ecosystem (Portielje et al. 1999). Eutrophication simply can be defined as nutrients enrichment leading to increased primary production (Chapman 1996) which can be natural or influenced by human activities.

Inland waters are important natural resources around the world; yet they are threatened by Eutrophication due to climate and anthropogenic changes, eutrophic waters are associated with the presence of various Phytoplankton species including cyanobacteria. Cyanobacteria are widely recognised for their negative impact on water quality, mainly due to the formation of surface scum and the ability to produce toxic substances. Therefore, the specific pigment of cyanobacteria, phycocyanin, and phytoplankton green pigment (chlorophyll-a) are the core discussion of this research in inland waters.

The use of earth observation data, specifically Medium Resolution Imaging Spectrometer (MERIS), combined with in-situ measurement is a reliable and affordable tool to monitor and predict Eutrophication in inland waters.

Inland waters are optically complex (Alikas et al. 2008) or case 2 waters (Gordon and Morel 1983) because they contain several uncorrelated constituents that contribute to the observed water leaving radiance. The optical properties of inland water have also high spatial and temporal variability which makes it more complex compared to case 1 waters.

MERIS is an appropriate sensor for this study because has spectral bands centred at 620, 650, 681 and 705 nm which allow estimation of absorption coefficients due to Phycocyanin pigment, an indicator of cyanobacteria, and Chlorophyll-a (Chl-a) in the presence of other constituents. It is easy to separate Phycocyanin pigment from other Phytoplankton pigments using MERIS. This is because Phycocyanin has a unique absorption peak at 620 nm (Bryant 1994;Yang et al. 2006) which correspond to MERIS band 6. Moreover MERIS has narrow bands and high radiometric sensitivity (Doerffer et al. 2007) which can detect low signal from these waters.

Eutrophication Index (E. I) can be calculated from a two variables, namely: nutrient (Nitrate, Nitrite, Ammonia, Phosphorus) and Chlorophyll-a (Primpas et al. 2009). These variables can be analyzed using multivariate techniques, e.g. principal component analysis, to produce an indicator on the trophic state of the water body. The method of Principal component analysis as proposed by Primpas et al.(2009) was implemented in this study combined with RS technique to compliment the development of multivariate index for assessing eutrophication. In turn this classification can be adapted to be in accordance with the European water framework directive.

Therefore; integration of these two approaches provided a realistic tool for monitoring and predicting Eutrophication in inland waters.

1.1. Research problem

Inland waters offer vast number of benefits ranging from recreational, economical as well as ecological; however they are prone to Eutrophication due to natural and manmade causes. Existing methods of monitoring eutrophication by in-situ measurements are not adequate due to the fact that it is not feasible to distribute sampling points all over the water body taking into consideration that water characteristics have high spatial and temporal variability. This is therefore a major setback when it comes to management and predicting eutrophication in inland waters. The lack of comprehensive methods for monitoring and predicting eutrophication is a problem and that shall be addressed by combining the use of MERIS data, bio-optic models and field based Eutrophication Index (E.I), a subject of this study.

1.2. Research Objective

The main objective of this research is to derive Remote sensing Eutrophication indicators maps from MERIS data, bio- optical modelling and compare Eutrophication Index derived from field data using multivariate analysis with Remote Sensed derive Eutrophication Index; however this will be achieved from the following specific objectives:

- Derivation of chlorophyll a and phycocyanin absorption coefficients from MERIS data as eutrophication indicators,
- Derivation of Eutrophication Index of inland water bodies using traditional measurement of water quality parameters,
- Derive Remote Sensed Eutrophication index,
- Compare In-situ derived Eutrophication index with Remote Sensed derived Eutrophication index,
- Validate the results.

1.3. Research questions

The major research questions to be addressed are:

- How can Chlorophyll a be derived separately with Phycocyanin pigments?
- How can RS-based Eutrophication index be established?
- Is it possible to replace In-situ derived E.I with Remote Sensed E.I?
- What is the Eutrophic status of the Roxo reservoir based on the developed method?
- What is the performance of the derived method?

1.4. Hypotheses

Inherent optical properties (IOP) can be derived separately from RS as Chlorophyll a and Phycocyanin absorption coefficients from simple inversion.

Remote Sensing Eutrophication Index (RS E.I) can be a good surrogate for In-situ derived E.I, and this can be used as a tool to facilitate implementation of European water framework directive.

1.5. Thesis structure

This thesis document is structured by chapters; Chapter one introduce brief literature review, research problem, objectives, questions and hypotheses. Chapter two gives in detail the concept of the thesis based on the existing literatures. Chapter three describe the study areas and used data set. In chapter four methods which have been used to meet the objectives are described. Chapter five is presenting the findings and contribution of the research in the scientific society. A complete discussion of the results is described in chapter six. Chapter seven contains the conclusions and recommendations of the thesis (Figure 1.5-1).

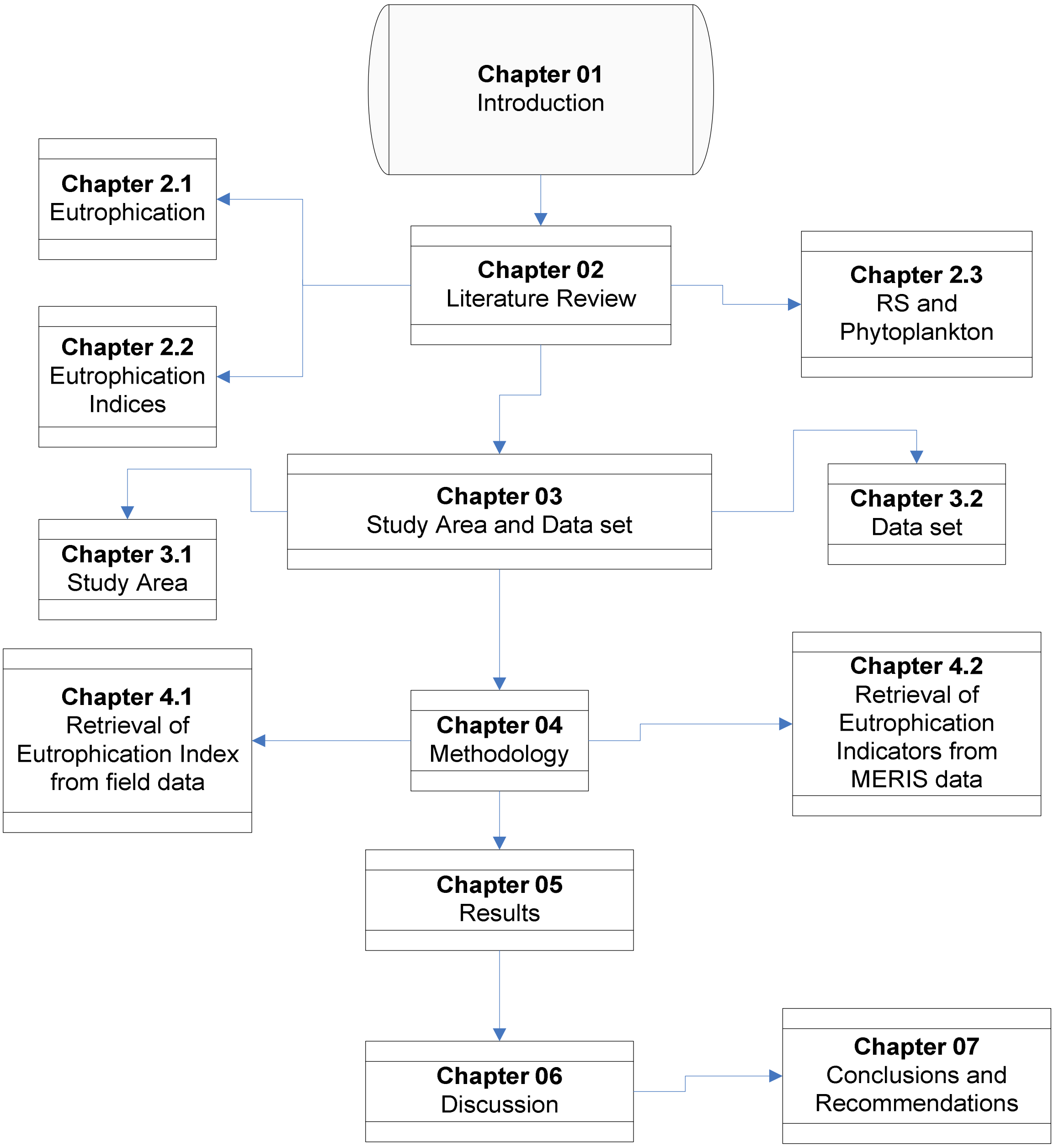

Figure 1.5-1: Thesis structure

2. Literature review

2.1. Eutrophication

Eutrophication has been defined in various ways; there is general agreement on the following definition of eutrophication (Tusseau-Vuillemin 2001;Bukata 2005;Khan et al. 2005): the nutrients enrichment from various sources (Figure 2.1-1) into water body together with other factors (temperature, light, oxygen, and retention time) causing increase in primary productivity of the ecosystem. Presence of eutrophication is commonly associated with greenish slim layer (Khan et al. 2005) which reduces light penetration as well as oxygen mixing which limit growth of other species in the water body. The process of eutrophication can be categorized into various trophic states as described hereunder:

- **Oligotrophic**; nutrients content in the water body is low and not productive in terms of aquatic animal and plant life,
- **Mesotrophic**; intermediate level of nutrients, fairly productive in terms of aquatic animal and plant life and showing emerging signs of water quality problems,
- **Eutrophic**; water body become rich in nutrients, very productive in terms of aquatic animal and plant life and showing increasing signs of water quality problems, and
- **Hypertrophic**; very high nutrient concentrations in the water body where plant growth is determined by physical factors; water quality problems are serious and almost continuous.

The above mentioned trophic states classification is well described in Table 2.1-1as adopted from Chapman (1996).

Eutrophication process can be natural or cultural (man made); natural eutrophication is caused by natural factors which will leads to nutrients enrichment to the water body, however this process is very slow and can not be regarded as threat, therefore cultural eutrophication which is the result of a rapid and excessive nutrients enrichment of water body (Tusseau-Vuillemin 2001) is of major concern. The key primary production process is photosynthesis which utilise solar energy, carbon dioxide, water, nitrate, phosphate, and other trace elements to produce phytoplankton (Cyanobacteria are among them) and dissolved oxygen as end product. External supply of nutrients will considerably increase the photosynthesis process keeping other factors constant, this situation will result into competition of resources amongst the species due to the increased population. Cyanobacteria (blue green algae) are very adaptive to critical conditions and will reproduce more and dominate phytoplankton biomass. Cyanobacteria domination leads to a decrease of biodiversity in the ecosystem (Tusseau-Vuillemin 2001) as well as producing toxic chemical (cyanotoxins) which is poisonous to humans and animals.

Table 2.1-1: Nutrient levels, biomass and productivity of lakes at each trophic category

Trophic Category	Mean TP (mg/m^3)	Annual mean chlorophyll (mg/m^3)	Chlorophyll maxima(mg/m^3)	Annual mean Secchi disc transparency (m)	Secchi disc transparency minima (m)	Minimum oxygen (% sat)[1]
Ultra-Oligotrophic	4.0	1.0	2.5	12.0	6.0	<90
Oligotrophic	10.0	2.5	8.0	6.0	3.0	<80
Mesotrophic	10- 35	2.5- 8	8- 25	6- 3	3- 1.5	40- 89
Eutrophic	35- 100	8- 25	25- 75	3- 1.5	1.5- 0.7	40- 0
Hypereutrophic	100.0	25.0	75.0	1.5	0.7	10- 0

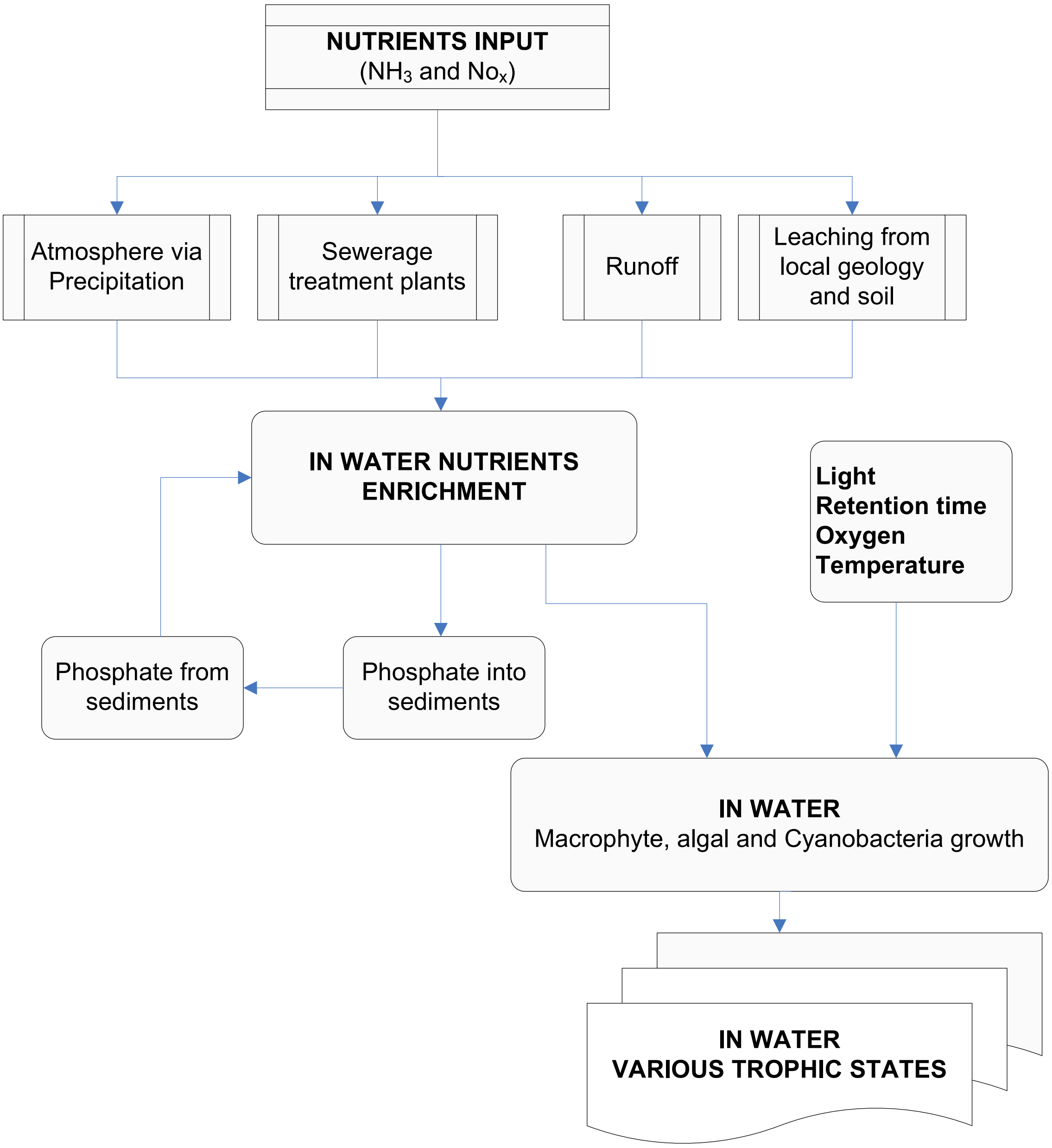

Figure 2.1-1: Eutrophication Causes

As mentioned before, light and temperature are two physical factors that can limit algal production but are not controlling factors due to the fact that tremendous algal production relies on the availability of nutrients. The elements needed for photosynthesis are commonly considered to be carbon (C), Hydrogen (H), Oxygen (O), and Phosphorous (P). Carbon, hydrogen and oxygen are readily available from the water and the atmosphere while nitrogen and phosphorous are not always available. Photosynthesis will be determined by the nutrient least available, this is called limiting nutrient, and *phosphorous* has been found to be the limiting nutrient and therefore human activities leading to increase of phosphorous concentration are the principal cause of eutrophication (Chapman 1996).

In normal clean water phosphorous concentration is very low to cause Eutrophication, so it needs external supply from various sources. Phosphorous concentration gets higher in the water bodies surrounded by agricultural, industrial or residential areas where by runoff from agricultural areas, chemical waste from industries and sewerage disposal from waste water treatment plants (Figure 2.1-1) are the major mechanisms for phosphorous input to these water bodies. Phosphorous does exist in various forms (dissolved and suspended) and the one responsible for Eutrophication is soluble inorganic phosphorous which is taken directly by plant cells (Khan et al. 2005), however any form added into water can be converted at the bottom of the water body and become soluble and available for Eutrophication. Overgrowth of phytoplankton has many negative effects (Figure 2.1-2) due to the fact that they will reduce light penetration, increase turbidity, decay and death will introduce toxic chemicals and recycle nutrients hence boosting Eutrophication. Therefore the process of Eutrophication increases with increase of phosphorous concentration, light intensity and temperature.

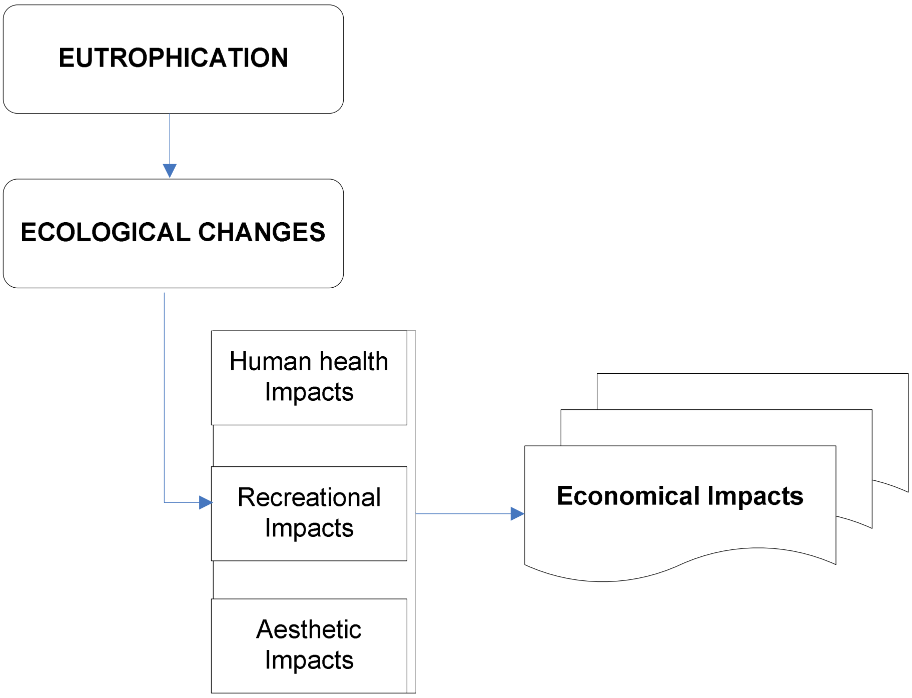

Figure 2.1-2: Eutrophication Impacts

2.2. Eutrophication Indices

Eutrophication status of a water body can be classified as Oligotrophic, Mesotrophic, Eutrophic and Hypertrophic but several factors have to be considered before doing the classification and therefore the process is multidimensional (Carlson 1977). Being multidimensional, multivariate technique is an appropriate approach for developing indices due to the fact that it incorporates several parameters which have influence to Eutrophication to classify a trophic state of the water body.

Eutrophication Index (E.I.) is among other Water Quality Indices (WQIs) which have been developed for aquatic ecosystem (Giordani et al. 2009), these WQIs can be developed based on the interest of the developer by selecting several water quality parameters of interest and apply multivariate technique like principal component analysis (PCA) (Primpas et al. 2009) to come up with multivariate indices. The indices are simple number ranges that have to be defined, like 1- 5 (Lacouture et al. 2006), 0- 100

(Giordani et al. 2009) depending on how the author wants to present it, however all the presentations have to be well defined to give actual presentation of the trophic state of the water body.

Chemical and biological parameters are all used to develop indices, therefore there is a need to make a relevant combination, and for this purpose multivariate technique can be used (Moncheva et al. 2002), some of the parameters used for determination of eutrophication indices are Dissolved oxygen (DO), Total phosphorous, Chlorophyll a concentration (Chl-a), Temperature, Secchi disc depth, Nitrate, Suspended particulate matters (SPM), and salinity.

Multivariate techniques are the statistical methods used to analyze simultaneous more than one variable on sample observations. These techniques can be grouped into two classes (Kothari 2004):

- For data containing both dependent and independent variables, and
- For data variables without dependency relationship

All above mentioned groups have their respective statistical methods to be applied and the methods can be identified by answering simple questions as summarized in the Figure 2.2-1 below (Sheth 1971):

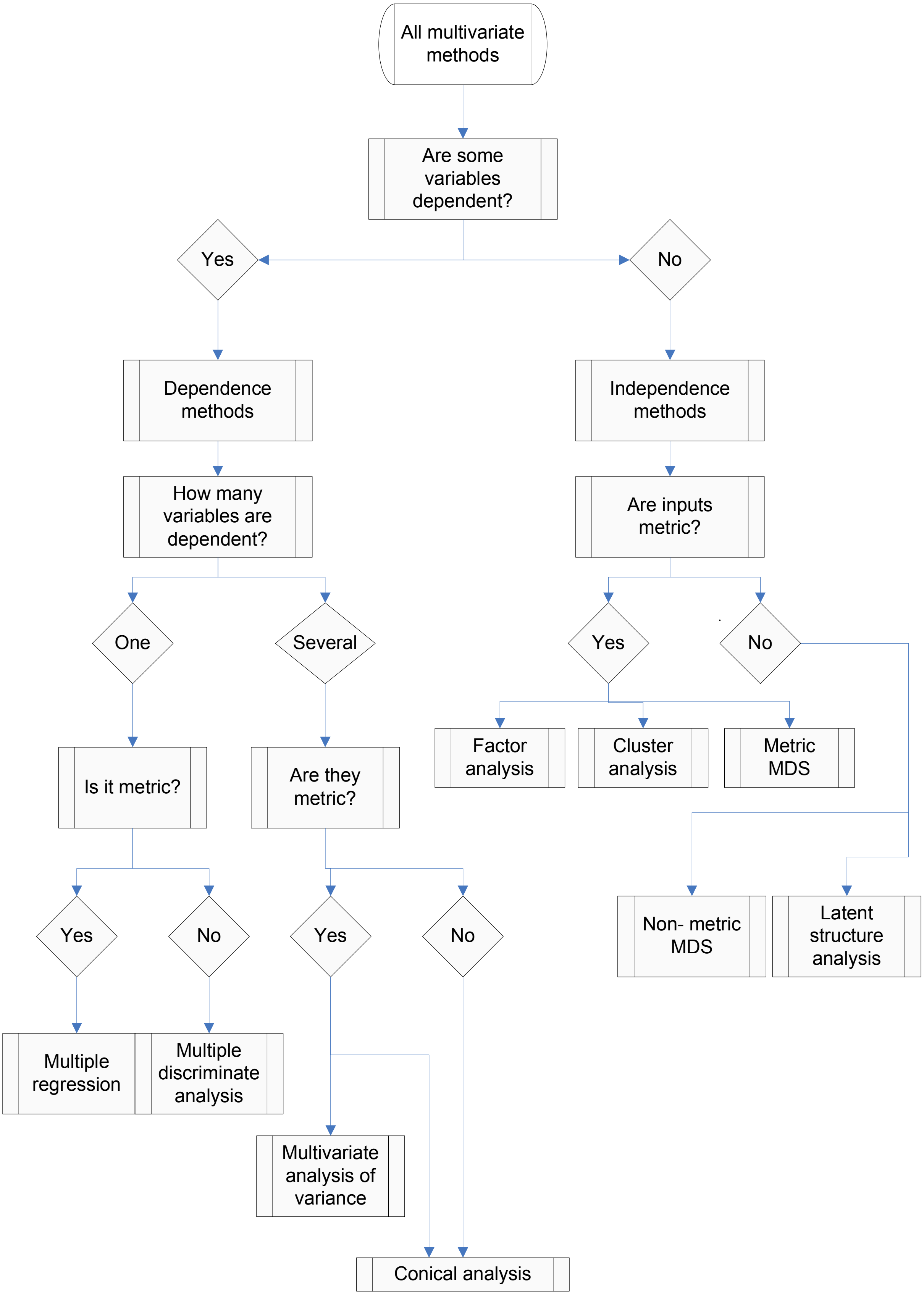

Figure 2.2-1: Classification of multivariate methods

Implementation of multivariate technique to get E.I will lead to classification of trophic status of water bodies of interest and therefore can be used as an input for implementation of the European Water Framework Directive (WFD); the directive was adopted on 2000 by European countries having a primary goal of ensuring availability of good water quality all over Europe. Among other requirements and targets of the directive; the determination of ecological status in European water bodies (Kagalou et al. 2009) is among them, and this achievement has to be attained by 2015 covering underground and surface waters. Integration of remote sensing technique assures the achievements of the directive and this is the contribution of this thesis towards the implementation of the directive.

2.3. Remote Sensing and Phytoplankton

Remote sensing technique can be used to monitor Phytoplankton biomass by means of sensor that is not in direct contact with the water body. Remote sensing techniques uses active or passive sensors to observe (taking images) water quality parameters (Bukata 2005), in this study passive sensor (MERIS) have been used. MERIS data are provided in two levels; level 1B data (L1B) which are not atmospherically corrected and level 2 data (L2) which are geolocated and atmospherically corrected.

MERIS onboard of ENVISAT satellite launched by European Space Agency (ESA) has spectral bands which are specifically designed for recording maximum absorption of phytoplankton pigments, chlorophyll-a and cyanobacteria (Simis et al. 2005 b) and these two species are the main focus of this thesis in terms of phytoplankton pigment. See Table 2.3-1 below summarizing characteristics of MERIS sensor (Bezy et al. 2000).

Table 2.3-1: MERIS Sensor Characteristics

Geometric Image Quality	
Field of View	68.5° centred about nadir
Swath width	1150 km
Localisation accuracy	<2 km (without the use of landmarks)
Spatial resolution	RR: 1040 m x 1200 m (nadir)
	FR: 260 m x 300 m (nadir)
Band to band registration	< 0.1 FR pixel
Spectrometric Image Quality	
Spectral range	390 nm- 1040 nm
Spectral sampling interval	1.25 nm
Spectral resolution	1.8 nm
Band transmission capability	15 bands centred at [412.5, 442.5, 490, 510, 560, 620, 665, 681.25, 708.75, 753.75, 760.625, 778.75, 865, 885 and 900 nm]

Band width	Programmable from 1.25 nm up to 30 nm
Band center knowledge	< 0.6 nm
Radiometric Image Quality	
Radiometric accuracy	< 2% in reflectance (i. e. relative to the sun irradiance)
Dynamic range	Up to bright clouds (100% reflectance)
Signal to noise ratio	1650 (@412.5 nm) for typical ocean signal
Polarisation sensitivity	< 0.3% over the full spectral range
Orbital signal stability	< 0.05%

Cyanobacteria also known as blue- green algae, blue- green bacteria or Cyanophyta is a phylum of bacteria that obtain their energy through photosynthesis, and able to harvest light for photosynthesis in a part of spectrum that is little used by other photosynthetic organisms which makes them to be more persistent in critical conditions. Cyanobacteria are oxygenic phototrophs which have continuous photo- synthesis growth in the presence of oxygen and use water as electron donor for carbon dioxide (CO_2) reduction (Chorus et al. 1999) and this unique character makes them to dominate in most of Eutrophic water bodies.

High cyanobacteria biomass presence in water is problematic caused by release of cyanotoxins which are harmful for aquatic organisms as well as humans; this has impact to the recreational value of the water body and ecosystem as well. Also cyanobacteria domination decrease the diversity of other phytoplankton species (Dokulil et al. 2000).

Eutrophic inland waters often exhibit blooms of cyanobacteria and remote sensing provides insights in the distribution of blooms for a large number of lakes or reservoirs simultaneously. Pigment phycocyanin (PC), which is characteristic of the presence of cyanobacteria can be detected from spectral reflectance which require more spectral information which could not be provided by satellite sensors with global coverage, therefore MERIS have been adopted for this assignments due to the following reasons (Simis et al. 2005 b):

- Band six at 620 nm includes the maximum absorption of a number of modifications of the PC pigment,
- 300 m spatial resolution is sufficient to monitor medium sized lakes and reservoirs, and
- Narrow spectral bands necessary to capture high variability of water characteristics.

At the moment there are three approaches which have been published to derive Phycocyanin pigment quantities from remote sensing data at 620 nm reflectance region (Ruiz-Verdú et al. 2008), these algorithms are:

- A single reflectance band ratio algorithm (Schalles et al. 2000),
- A semi-empirical baseline algorithm (Dekker 1993), and
- A nested semi- empirical band ratio algorithm (Simis et al. 2005 b).

From the above list, a nested semi- empirical (Simis et al. 2005 b) was found to be the best in eutrophic waters (Ruiz-Verdú et al. 2008) and was developed for MERIS band setting and therefore tested in this research.

Chlorophyll a and Cyanobacteria do exist together in the Phytoplankton blooms with varying concentration and difference spectral characteristics, their variation in spectral characters can be determined using MERIS sensor because they have different absorption peaks.

Therefore MERIS full resolution images have been used in this research to derive Chlorophyll a and Phycocyanin absorption coefficients separately.

3. Study Area and Data set

3.1. Study area

The study area for this MSc research is Roxo reservoir in Portugal. Roxo reservoir is located in southern part of Portugal in Beja district within Outeiro catchment with the geographical location of $37^0 55'48''$ N and $8^0 6'9''$W (see Figure 3.1-1). It has surface area of 13.8 km^2, elevation of 122.5-280 m above mean sea level (a.m.s.l) and its surface area varies with seasonal changes; increasing during rain season and decreasing during dry season. Water quality of the reservoir is mainly altered by agricultural runoff as well as pollution point source from waster water treatment plants. The land use of the surrounding catchment is mainly agricultural.

Roxo catchment has area coverage of 353 km^2 (Sen et al. 2005), as mentioned earlier that the main land use in this catchment is agricultural with dominant crops of cereal and sunflower while corn is the alternative crop during dry seasons (Paralta et al. 2005). At the catchment there also other crops cultivated which include tomatoes, olives, rice and grapes (Gamises 2009).

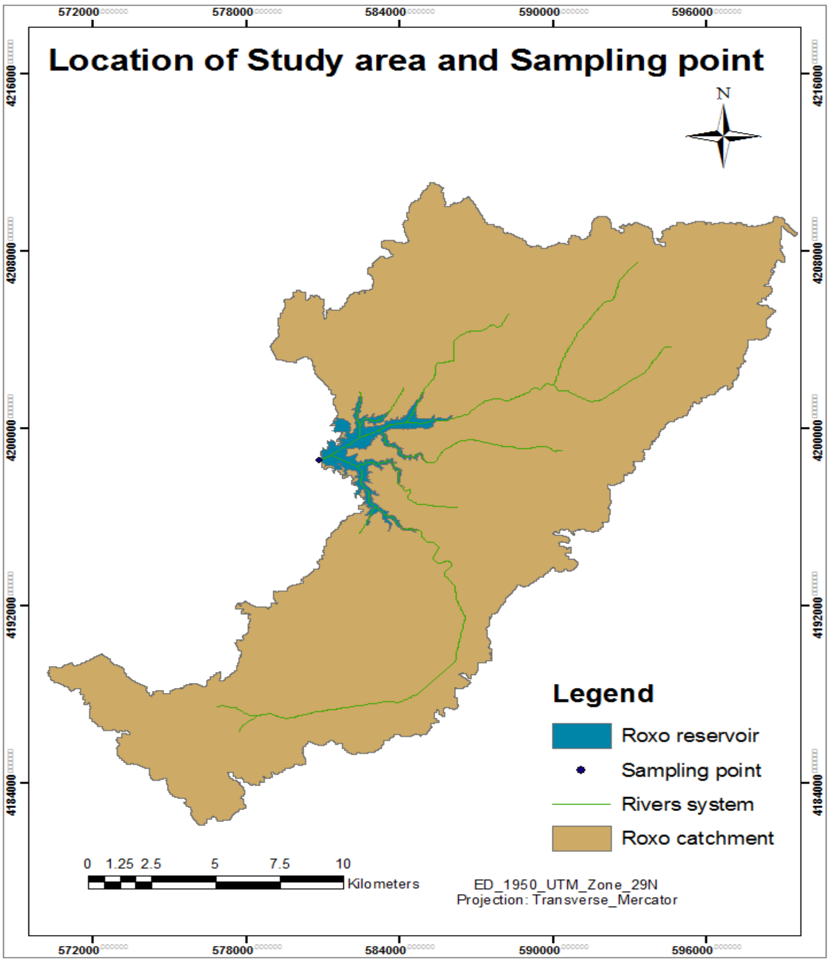

Figure 3.1-1: Map showing Roxo reservoir

Climatic condition of Portugal is mainly maritime temperate; however, the project area is dominated by Mediterranean climate which is influenced by Atlantic Ocean and is warmer and drier than other parts of the country (Sen et al. 2005).

The area has the average precipitation of 587 mm per year with mean maximum and minimum air temperature of 33^0 and 6^0C in the month of July and January respectively according to the data records of 1961 to 1990 (Pascal 2008).

According to the daily data for air temperature and precipitation obtained from SAGRA (Agro meteorological System for the Management of Irrigation in the Alentejo) from the year 2005 to 2008, maximum and minimum daily air temperature is 24.56 and 9.65^0C respectively, and average daily rainfall is 1.39 mm (Figure 3.1-2;Figure 3.1-3 and Figure 3.1-4).

Surrounding Roxo reservoir, four soil classes are identified according to FAO- UNESCO soil classification namely; Litossols, Luvissols, Planossols and Vertissols (Sen et al. 2005). Its catchment has a gentle slope heading west with the elevation varying from 24 5 m a.m.s.l (highest) to 125 m a.m.s.l (lowest) (Vithanage 2009).

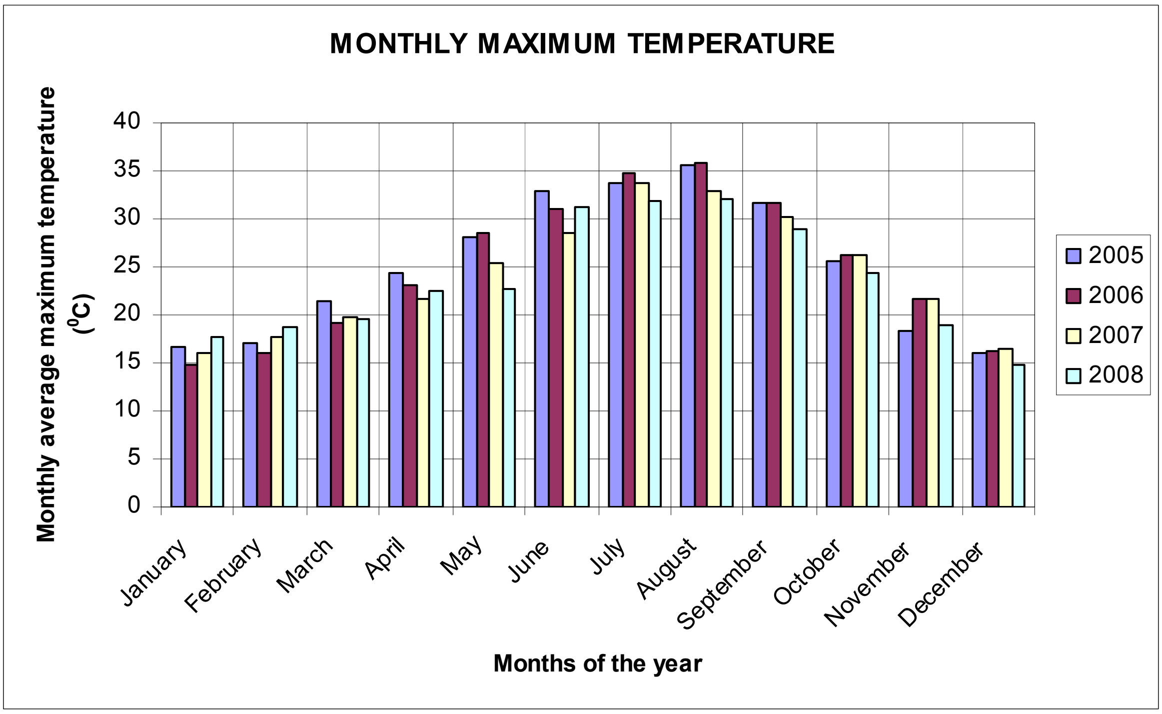

Figure 3.1-2: Monthly maximum temperature (^{0}C)

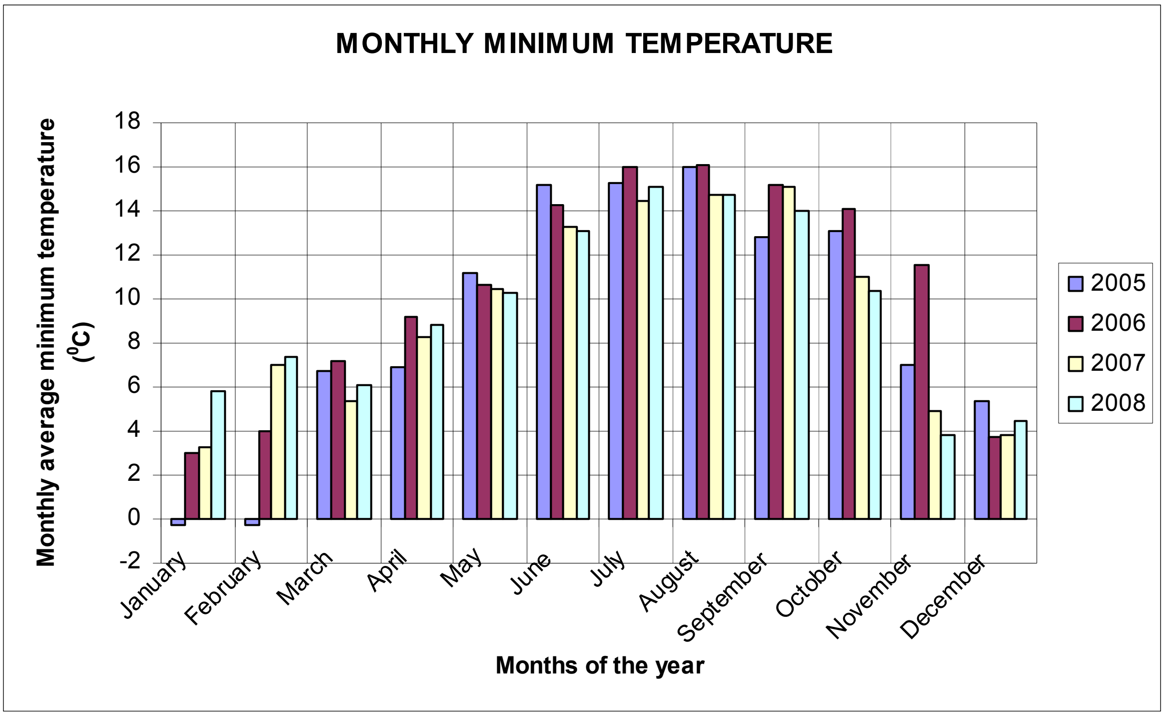

Figure 3.1-3: Monthly minimum temperature (^{0}C)

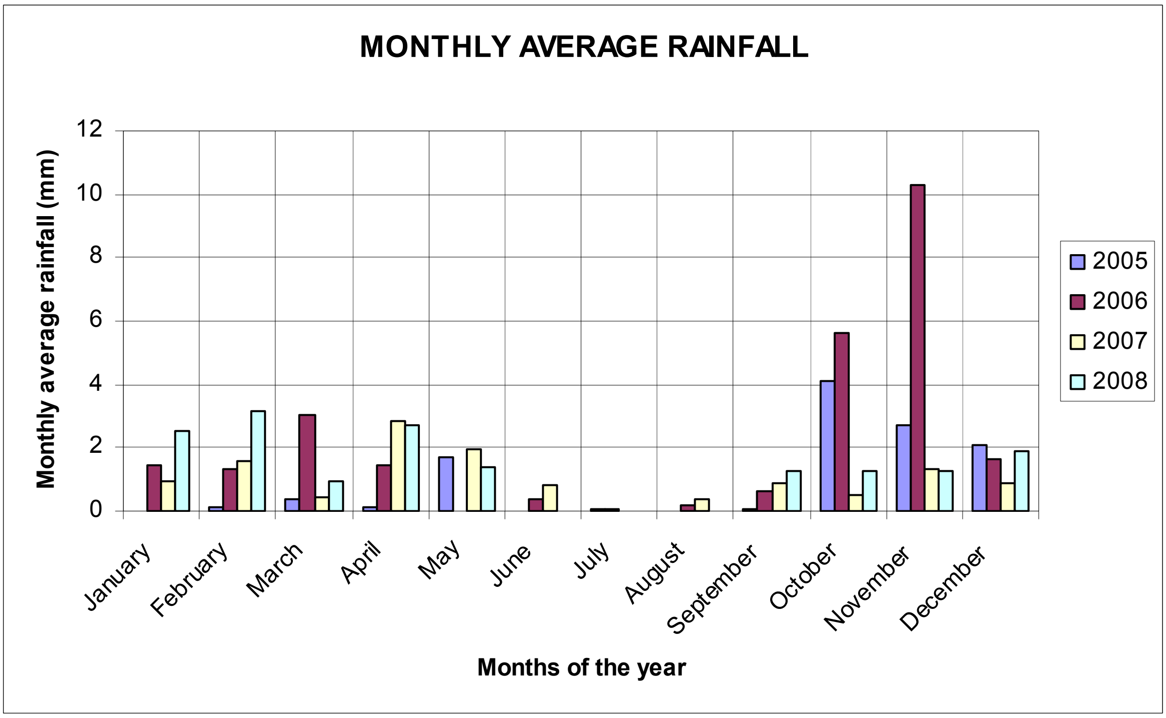

Figure 3.1-4: Monthly average rainfall (mm)

3.2. Data set

Good data availability is a constraint in this research, as it will be noted in the following chapters; therefore, various data from different places had to be used for demonstration and validation of the derived analytical model. The following list below shows type of data used and their purposes:

- Poyang Lake MERIS image (dated 16th October 2008) for derivation of model outputs,
- Poyang Lake in-situ water quality measurements for validation of derived parameters,
- Bohai sea MERIS image (dated 14th February 2004) for clear demonstration of the outputs of the proposed model,
- Roxo reservoir MERIS images (dated 02nd October 2006 and 29th May 2007) for derivation of model outputs in the study area and derivation of remote sensing eutrophication index,
- Roxo reservoir in-situ water quality measurements for derivation of in-situ eutrophication index.

Poyang Lake and Bohai sea mentioned above are all located in China. Nevertheless, the project area remains to be Roxo reservoir in Portugal and its data selection and ordering is given in brief in the following paragraphs.

Insitu water quality data were selected from two data sets available at ITC water department, first set covers year 2002 up to 2005 and the second set covers year 2005 up to 2008, however, the second data set (2005- 2008) was used because it has significant number of water quality parameters relevant for Eutrophication than the first set and it has more MERIS images corresponding to the sampling dates of the water quality parameters which is necessary for validation (Table 3.2-1).

MERIS images full resolution (FR) are available from European Space Agency (ESA), the images have been selected using The European space agency's multi- mission, catalogue and ordering services (EOLISA), see image's metadata in the Table 3.2-1. The selection of available full resolution images based on the following:

- Cloud coverage of the image, only cloud free were selected, and
- Image acquisition date has to correspond to the date of water quality measurements.

Table 3.2-1: Characteristics of data available

Water Quality data	**Measured parameters**
2005- 2008	Nitrates
	Total Phosphorus
	Nitrites
	Ammonia
	Chlorophyll a
2002- 2005	Phosphates
	Chlorophyll-a
MERIS FR data	**Metadata of Available images**

2005- 2008	MERIS_FR1P_20050111_100000
	MERIS_FR1P_20060626_095000
	MERIS_FR1P_20061002_120000
	MERIS_FR1P_20070529_111000
	MERIS_FR1P_20071029_113000
	MERIS_FR1P_20071127_100000
2002- 2005	MERIS_FR1P_20031007_100000
	MERIS_FR1P_20040406_100000

The criteria mentioned above for MERIS image selection is necessary because cloud free images were needed for this assignment. The dates of images in Table 3.2-1 corresponds to in-situ water quality data (see appendix B). Therefore both data sets for the year 2005 up to 2008 for Insitu water quality measurements and corresponding MERIS images were used to achieve proposed objectives.

4. Methodology

4.1. Retrieval of Eutrophication Index from in-situ measurements

Water quality data from 2005 to 2008 for Roxo reservoir have been used to determine Eutrophication index in the reservoir. The following water quality parameters were measured:

- Phosphorous (PO_4),
- Nitrates (NO_3),
- Nitrites (NO_2),
- Ammonia (NH_3), and
- Chlorophyll-a concentration.

Eutrophication was identified and categorized by the concentration of chlorophyll a in the water bodies; Eutrophication needs Nitrate and Phosphorous as key nutrients assuming temperature and light are naturally available and cannot be controlled. In this context chlorophyll a is criterion variable since depend on nitrate and phosphorous while the two mentioned are explanatory variables since they cause Eutrophication to occur.

Based on the classification of multivariate methods (Sheth 1971) multivariate analysis of variance have been used to develop the relation between Eutrophication occurrence and chlorophyll a concentration and nutrients presented by Eutrophication indices (E.I). The method of Principal Component Analysis (PCA) was used and the equation developed by Primpas et al. (2009) was adopted in this thesis. The equation is expressed as follows:

$$E.I = a_1 C_{PO4} + a_2 C_{NO3} + a_3 C_{NO2} + a_4 C_{NH3} + a_5 C_{chl-a} \qquad (4.1\text{-}1)$$

The above stated equation (4.1-1) has coefficients of the first principal component for the five variables which are a_1, a_2, a_3, a_4, and a_5 and C stand for concentration of respective variable as shown. As it can be noted from appendix B, data range differs greatly between variables therefore coefficients (a_i) were obtained after standardization which was done by calculating principal component using correlation matrix (Rencher 2002) by principal component (pcomp) function as Interactive Data Language (IDL) code.

Therefore, equation 4.1-1 was applied on the In-situ water quality measurements (appendix B) to calculate Eutrophication Indices of Roxo reservoir and compare them with the RS derived indices.

4.2. Retrieval of Eutrophication Indicators from MERIS data

In this context, Eutrophication indicators are Chlorophyll a and Phycocyanin pigments. To retrieval above mentioned indicators, full resolution (FR) MERIS images have been used to retrieve absorption coefficients due to Chlorophyll a and Phycocyanin as well and relate these coefficients with their respective pigments concentrations. The retrieval process involved the following steps listed hereunder and summarized in Figure 4.2-1:

- Atmospheric correction of the images, which was done as stipulated by Doerffer et al. (2008), see appendix C for details,
- Application of the empirical model of Simis et al. (2005 b) to retrieve absorption coefficient due to Phycocyanin (a_{pc}), this is empirical model and it was found to be valid for the used data set only, see appendix D for the details of the model,
- Derive a simple inversion (analytical approach) to retrieve a_{pc} and combine it with modified GSM01 model to derive Chlorophyll a concentration, $a_{dg}(440)$, $b_{bp}(440)$ and $a_{pc}(620)$.

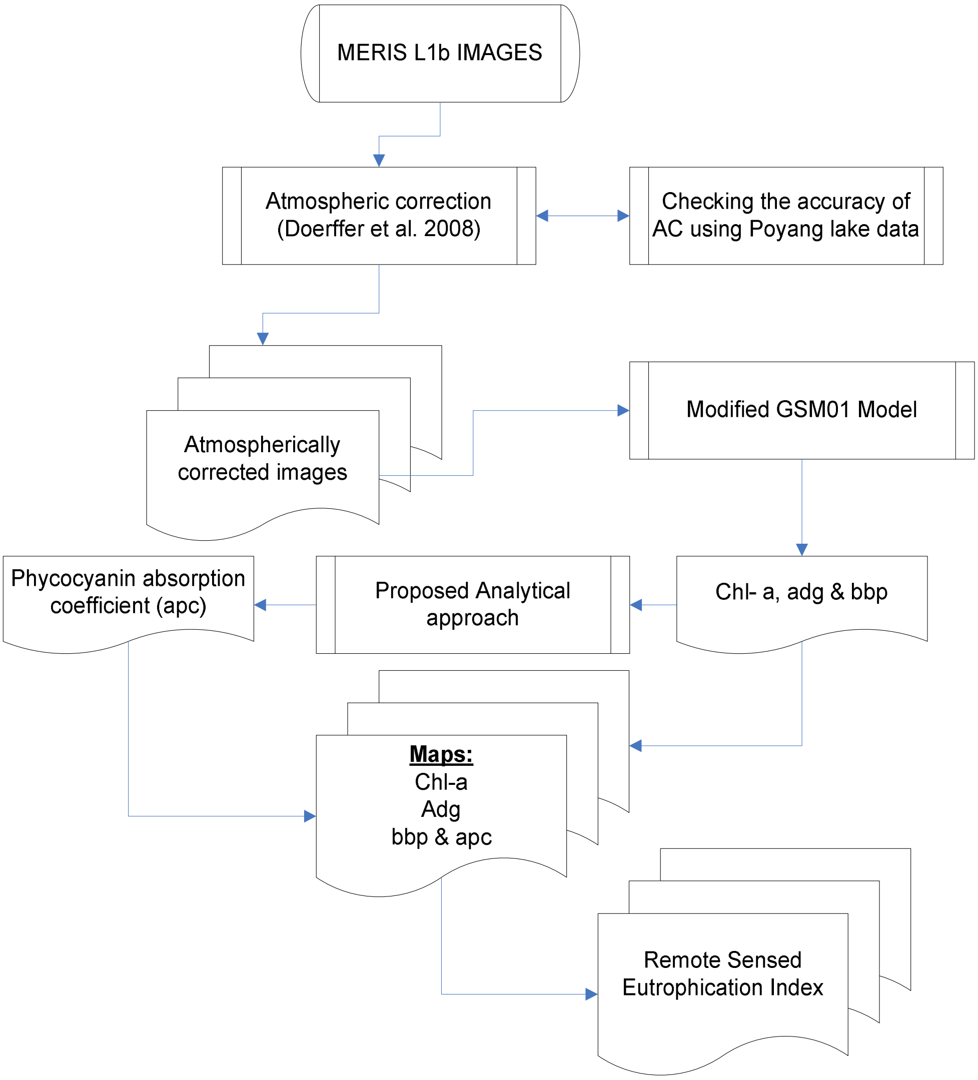

Figure 4.2-1: Summary of proposed approach

4.2.1. Retrieval of Eutrophication indicators using modified GSM01 model and derived simple inversion

The first concept of this research was to use the model of Simis et al. (2005 b) to derive absorption coefficients due to phycocyanin pigment and their concentration, however the model (Simis et al.

2005 b) gave negative values for most of the PC concentration and therefore proved to be not applicable for our data (see appendix D for the details on the model). This model failure can also be attributed by introduction of correction and conversion factors which were obtained from a specific data set. Therefore, this thesis is introducing analytical approach to derive absorption coefficient due to Phycocyanin pigment at the wavelength of 620 nm and Chlorophyll- a absorption coefficients by modifying GSM01 model by removing band 6 (620 nm). Taking into consideration that absorption peak of phycocyanin is around 620 nm (Bryant 1994;Yang et al. 2006) which make it possible to be isolate from other Phytoplankton species, therefore Gordon model (Gordon 1976;Gordon et al. 1988a;Maritorena et al. 2002) has been used in modified GSM01 model to retrieve Chlorophyll a concentration, absorption coefficient due to dissolved organic matter and backscattering coefficient due to particulate matters and use them as input to a simple derived inversion to retrieve absorption coefficient due to phycocyanin pigment at 620 nm.

In-situ water quality measurements and MERIS matchup full resolution images were used in this thesis, the images were atmospherically corrected according to Doerffer et al.(2008) as described in appendix C Water leaving irradiance reflectance of 12 bands (1-10, 12 and 13) as a result of atmospheric correction process was used for retrieval of eutrophication indicators.
However, resulted images from atmospheric correction process had to be masked to separate land from water pixels. Relation by Gordon et al. (1988b) was used and an assumption that water body under consideration will have maximum turbidity so as to derive maximum water leaving reflectance for masking was made, the second component of right hand side of equation 4.2-1 become equal to one and therefore Rsw is equal to *f* which gave the maximum value of 0.16 and finally mask was built using 0 as minimum and 0.16 sr^{-1} as maximum water leaving reflectance and was applied to all images.
The retrieval process involved two main steps, namely:

- Retrieving Chl-a concentrations from the image as a general phytoplankton indicator, excluding the phycocyanin band at 620 nm using modified GSM01 model and
- Using the estimated values of Chl-a, a_{dg} and bb_p from the first step, in equation 4.2-1 to derive the absorption coefficient of phycocyanin pigments at 620nm [apc (620)].

Chlorophyll a concentration was derived using modified GSM01 model as one of the indicator of eutrophication, in this process the original GSM01 model (Maritorena et al. 2002) was edited by excluding band 6 (620 nm) to ensure that cyanobacteria is isolated from calculated Chlorophyll a concentration.

Absorption coefficient of phycocyanin pigment at 620 nm was calculated from derived analytical approach which uses the outputs from modified GSM01 model as its inputs. The analytical approach proposed in this research uses the same main Gordon et al. (1988b) relation (see equation 4.2-1) as Simis model, however, Simis model used only single geometrical factor (g_i) which made the model to be slightly simple. In this case both geometrical factors (g_1 and g_2) were taken into consideration because case II waters are optically complex. Considering Gordon et al. (1988b) below:

$$\mathrm{Rs}_{\mathrm{w}}(\lambda) = \frac{t}{n_{\mathrm{W}}^{2}} \sum_{i=1}^{2} g_i \left(\frac{b_b(\lambda)}{a(\lambda) + b_b(\lambda)} \right)^{i} \qquad (4.2\text{-}1)$$

In equation 4.2-1 above, the values of t, and n_w are constant adopted from Maritorena et al. (2002) and g_1 and g_2 are obtained as the result of Monte Carlo simulation (Gordon et al. 1988b).

The two inherent Optical Properties (IOPs) in equation 4.2-1 namely; bulk backscattering and absorption coefficients [$b_b(\lambda)$ and $a(\lambda)$] are divided into their contributing components as follows:

$$a(\lambda) = a_w(\lambda) + a_{ph}(\lambda) + a_{dg}(\lambda) \qquad (4.2\text{-}2)$$

Bulk absorption coefficient in equation 4.2-2 above is the result of absorption coefficients of the three contributing components which are water molecules (w), phytoplankton (ph) and dissolved organic matters (dg).

$$b_b(\lambda) = b_{bw}(\lambda) + b_{bp}(\lambda) \qquad (4.2\text{-}3)$$

Bulk backscattering coefficient in equation 4.2-3 above is contributed by backscattering coefficients due to water molecules (w) and particulate particles (b_{bp}).
Absorption and backscattering coefficient due to water molecules (a_w and b_{bw}) are obtained from Pope et al.(1997) and Smith et al.(1981) respectively.

The IOPs derived from equation 4.2-1 are a_{chl}, b_{bp}, and a_{dg}, during this process band 6 (620nm) was excluded in the processing so as to remove the contribution from Phycocyanin pigment.

Considering the maximum absorption of Phycocyanin pigment is at 620 nm and neglecting elsewhere made it possible to isolate phycocyanin absorption from other phytoplankton species. Therefore at 620 nm absorption due to Phycocyanin is dominant and bulk absorption coefficient will also include absorption coefficient due to phycocyanin (a_{pc}) as follows:

$$a(620) = a_w(620) + a_{chl}(620) + a_{dg}(620) + a_{pc}(620) \qquad (4.2\text{-}4)$$

Absorption due to detritus and dissolved organic matters are combine together because they have the same spectral shape (Maritorena et al. 2002), and at 620 nm can be expressed according to Bricaud et al.(1981) as follows:

$$a_{dg}(620) = a_{dg}(440)\exp[-S(620-440)] \qquad (4.2\text{-}5)$$

Referring to the bulk backscattering coefficient [$b_b(\lambda)$] in equation 4.2-3, b_{bw} is known (Smith et al. 1981), only b_{bp} is unknown and at 620 nm can be expressed according to (Maritorena et al. 2002), as follows:

$$b_{bp}(620) = b_{bp}(440) * \left(\frac{620}{440}\right)^{-\eta} \qquad (4.2\text{-}6)$$

Spectral decay constant (S) and power law exponent for the particulate backscattering coefficient (η) in equations 4.2-5 and 4.2-6 are adopted from Maritorena et al. (2002) as 0.0206 nm^{-1} and 1.03373 respectively.

At 620 nm, the equation 4.2-1 (Gordon et al. 1988b) can be re-written as follows;

$$\mathrm{R}_{\mathrm{sw}}(620) = \frac{t}{n_w^2} g \frac{b_b(620)}{a(620) + b_b(620)} \qquad (4.2\text{-}7)$$

All IOPs at 620 nm (b_b and a) have been expanded and explained sufficiently to be used to derive a_{pc} from remote sensing reflectance leaving water surface (R_{sw}), therefore equation 4.2-7 can be rearranged as follows:

$$\mathrm{a}(620) = b_b(620)\left(\frac{f}{R_{sw}(620)} - 1\right) \qquad (4.2\text{-}8)$$

Where, $f = gt/n_w^2$, the two equations, 4.2-8 and 4.2-4 can be combined and leads to the following relationship;

$$b_b(620)\left(\frac{f}{R_{sw}(620)} - 1\right) = \mathrm{a}_{\mathrm{w}}(620) + \mathrm{a}_{\mathrm{chl}}(620) + \mathrm{a}_{\mathrm{dg}}(620) + \mathrm{a}_{\mathrm{pc}}(620) \qquad (4.2\text{-}9)$$

Finally $a_{pc}(620)$ can be derived from equation 4.2-9 as follows:

$$\mathrm{a}_{\mathrm{pc}}(620) = b_b(620)\left(\frac{f}{R_{sw}(620)} - 1\right) - \left[\mathrm{a}_{\mathrm{w}}(620) + \mathrm{a}_{\mathrm{chl}}(620) + \mathrm{a}_{\mathrm{dg}}(620)\right] \qquad (4.2\text{-}10)$$

It can be noted that all the components of the right side of equation 4.2-10 have been explained except for absorption coefficient due to chlorophyll a at 620 nm [$a_{chl}(620)$] which is derived according to Lambert beer's law as follows:

$$a_{chl}(620) = Chl \times a^*{}_{chl}(620) \qquad (4.2\text{-}11)$$

Chlorophyll a concentration (Chl) in equation 4.2-11 was also derived from the modified GSM01 model.

Therefore equations 4.2-5, 4.2-6, 4.2-10 and 4.2-11 were written together with modified GSM01 as a code in Interactive Data Language (IDL) format and applied for the entire images to generate a map with four bands (three bands which are Chl, a_{dg} and b_{bp} are products of modified GSM01 model excluding band six, while the fourth band of a_{pc} is the output of developed analytical approach) as listed hereunder:

- Band 1- Chlorophyll a concentration (mg/m^3),
- Band 2- Absorption coefficient due to dissolved organic matters [$a_{dg}(440)$ m^{-1}],
- Band 3- Backscattering coefficient due to particulate matters [$b_{bp}(440)$ m^{-1}], and

- Band 4- Absorption coefficient due to phycocyanin pigments [$a_{pc}(440)\ m^{-1}$].

The output maps were visualized and customized to show distribution of all mentioned water quality parameters. Insitu measurements for Chlorophyll a concentration and Suspended Particulate Matters (SPM) were used for validation. Phycocyanin pigments have been presented by absorption coefficients only because its concentration increase with increase of absorption coefficients and specific absorption coefficients of Phycocyanin are very site specific therefore they were not considered in this case.

Remote sensed derived water quality maps (Figure 4.2-1) were used to develop Remote sensed Eutrophication Indices (R.S.E.I.) and compare it with Eutrophication indices (E.I.) derived from water quality in-situ measurements to investigate the possibility of R.S.E.I. to replace E.I. see Figure 4.2-2 below:

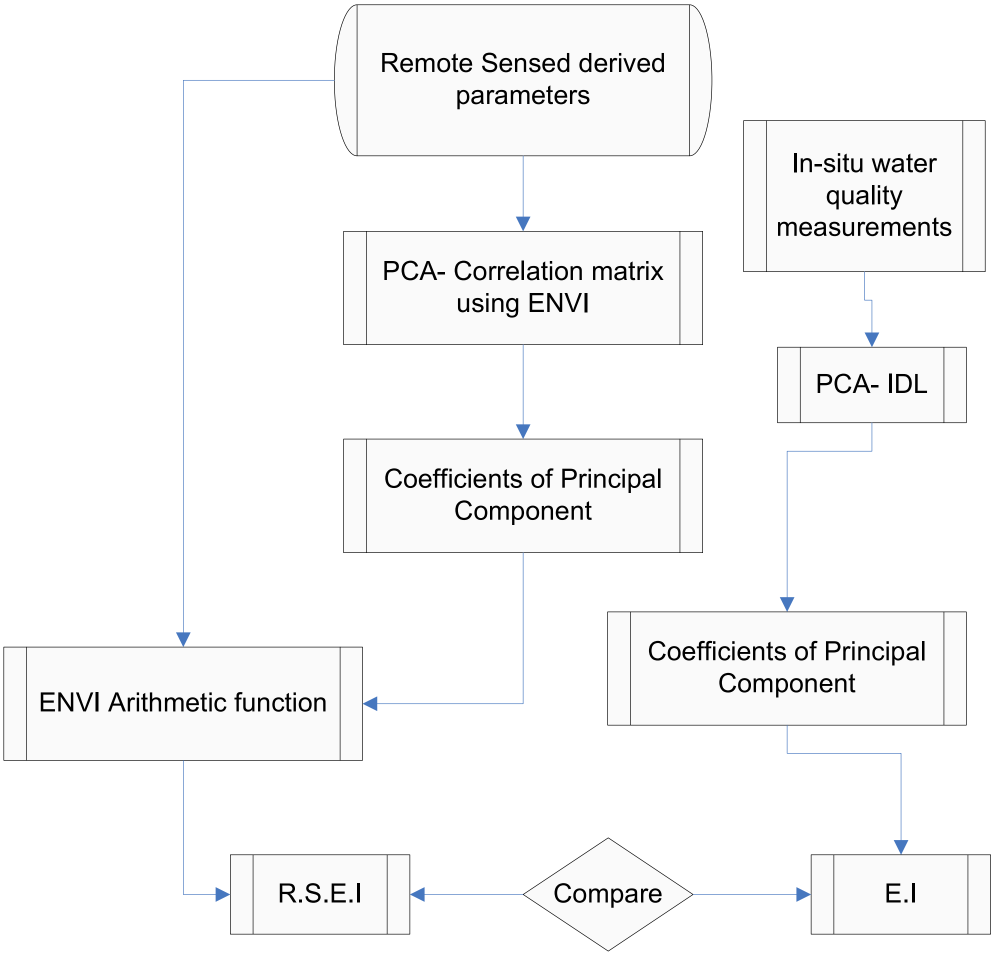

Figure 4.2-2: Eutrophication Indices development and comparison

5. Results

5.1. Atmospheric correction

In retrieval of water quality parameters from images, atmospheric correction had to be done before any further processing to remove the effect of atmosphere on final results. The accuracy of atmospheric correction method used (Doerffer et al. 2008) on level 1b MERIS images was checked using available data for Poyang Lake in China; In-situ water leaving reflectance measurements taken on 19th October 2008 were compared with corresponding imagery derived reflectance after atmospheric correction (Doerffer et al. 2008) and gave good correlations having R^2 ranging from 0.8722 to 0.9342 (Figure 5.1-1).

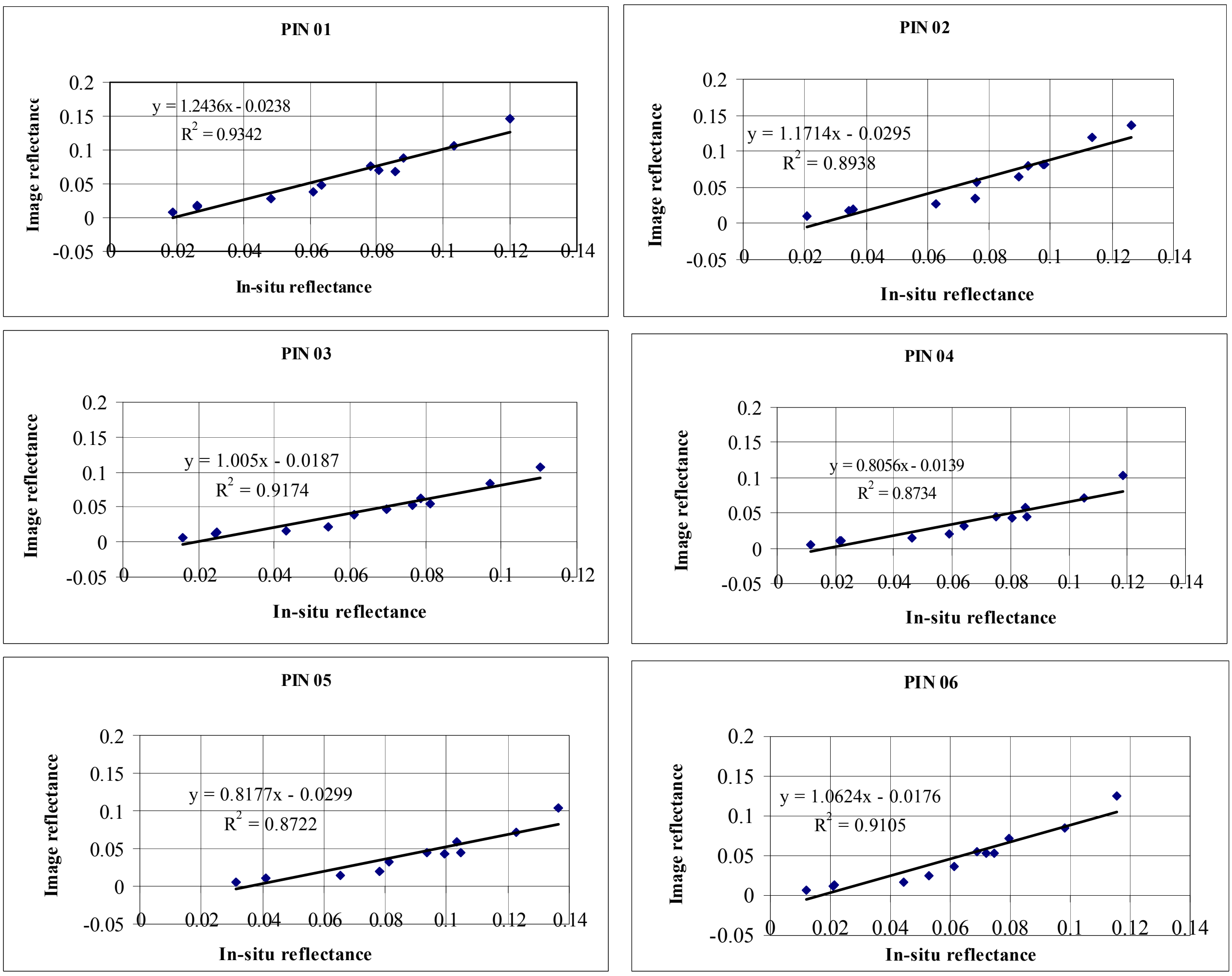

Figure 5.1-1: Accuracy of Atmospheric correction method

5.2. Water quality parameters derived from Poyang lake

Derived analytical method was applied on Poyang Lake to retrieve all four parameters and validate derived Chlorophyll a and SPM using in-situ measured concentrations. Specific absorption coefficient of Chlorophyll a derived by Xichang (2009) which is 0.0551 m^2/mg for Poyang Lake was used to convert absorption to concentration. The derived maps are shown in Figure 5.2-1 below:

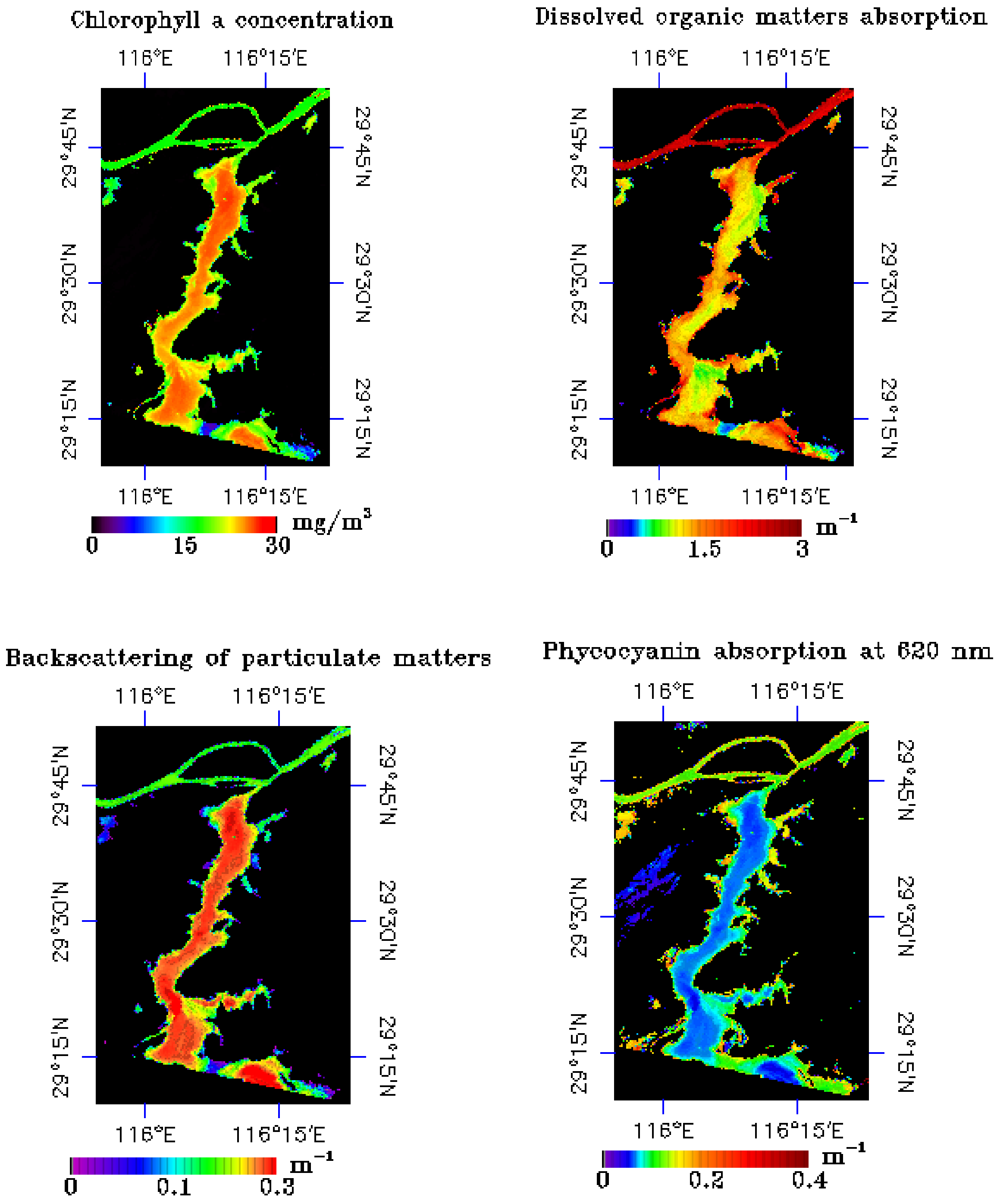

Chlorophyll a concentration

Dissolved organic matters absorption

Backscattering of particulate matters

Phycocyanin absorption at 620 nm

Figure 5.2-1: Derived water quality parameters for Poyang lake

5.2.1. Validation of the method using Poyang Lake data

In-situ water quality measurements from Poyang Lake were used for validation of derived analytical method. There were 30 in-situ measurement points, however during validation only 6 points were considered because these are the only points coinciding with in-situ measurement date. The validation was done for both chlorophyll a concentration and suspended particulate matters (SPM) as can be seen in Table 5.2-1 and Table 5.2-2 below. During validation, those 6 image matching points were extracted and their values were adjusted to correct for atmospheric transmittance. The factor Q (ratio of irradiance reflectance to remote sensing reflectance) was set as 2.5 sr (Albert et al. 2003) and used to relate reflectance and remote sensing reflectance. Corrected points were used to retrieve chlorophyll a and SPM for validation. Because of having fewer number of validation points it was not possible to present them graphically. Validation results gave relative errors (R.E) ranging from 18% to 33% for chlorophyll a concentration; and 9% to 32% for SPM.

Table 5.2-1: Validation results for Chlorophyll a concentration

Insitu measured (mg/m^3)	Chlorophyll a absorption (m^{-1})	Derived Chl a (mg/m^3)	R.E (%)
0.215	0.242	0.269	24.951
0.711	0.310	0.854	20.112
1.189	0.294	0.810	-31.828
0.806	0.238	0.654	-18.789
0.808	0.238	0.654	-18.990
0.999	0.240	0.661	-33.801

Table 5.2-2: Validation results for SPM concentration

Insitu measured (mg/l)	Backscattering (m^{-1})	Derived SPM (mg/l)	R.E (%)
36.000	0.447	32.707	-9.149
31.333	0.561	41.020	30.916
22.000	0.345	25.219	14.633
27.600	0.255	18.647	-32.439
27.600	0.255	18.647	-32.439
17.000	0.299	21.841	28.478

5.2.2. Method testing using Poyang Lake data

Derived method when applied on an image four products are obtained; namely Chlorophyll a concentration, backscattering coefficients due to particulate matters, absorption coefficients due to dissolve organic matters and phycocyanin pigments. In a bloom of phytoplankton, chlorophyll a and phycocyanin do exist together. The coexistence of these species has been used to test reliability of derived model. Figures below (Figure 5.2-2, Figure 5.2-3 and Figure 5.2-4) show their relationships between phycocyanin and chlorophyll a at different stages:

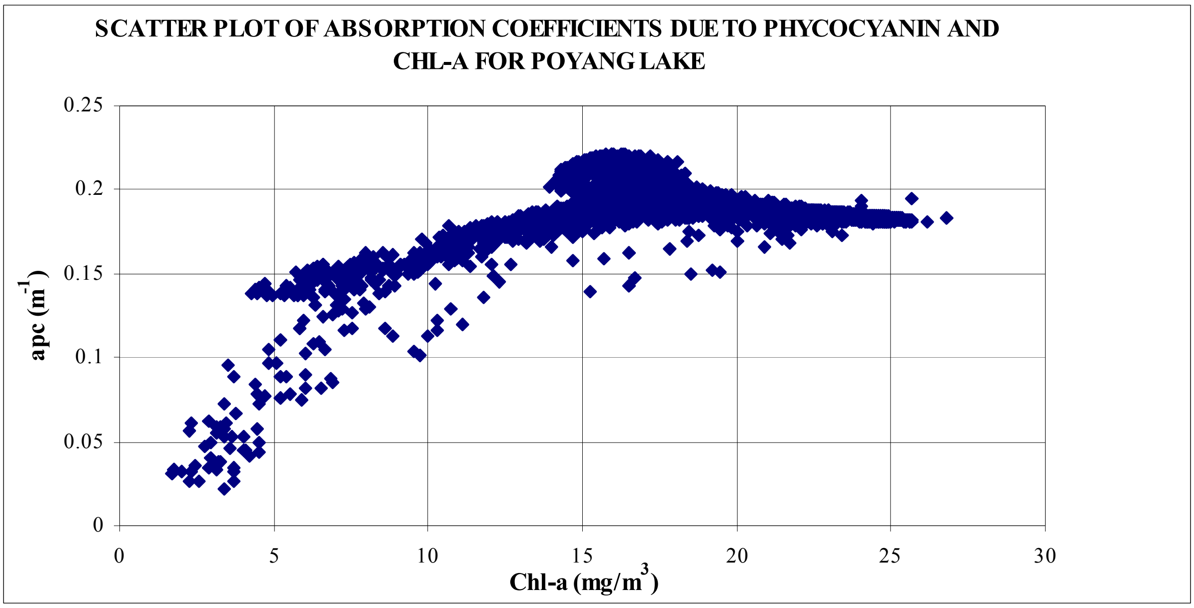

Figure 5.2-2: Relationship between Phycocyanin absorption coefficients and Chlorophyll a concentration for entire scene

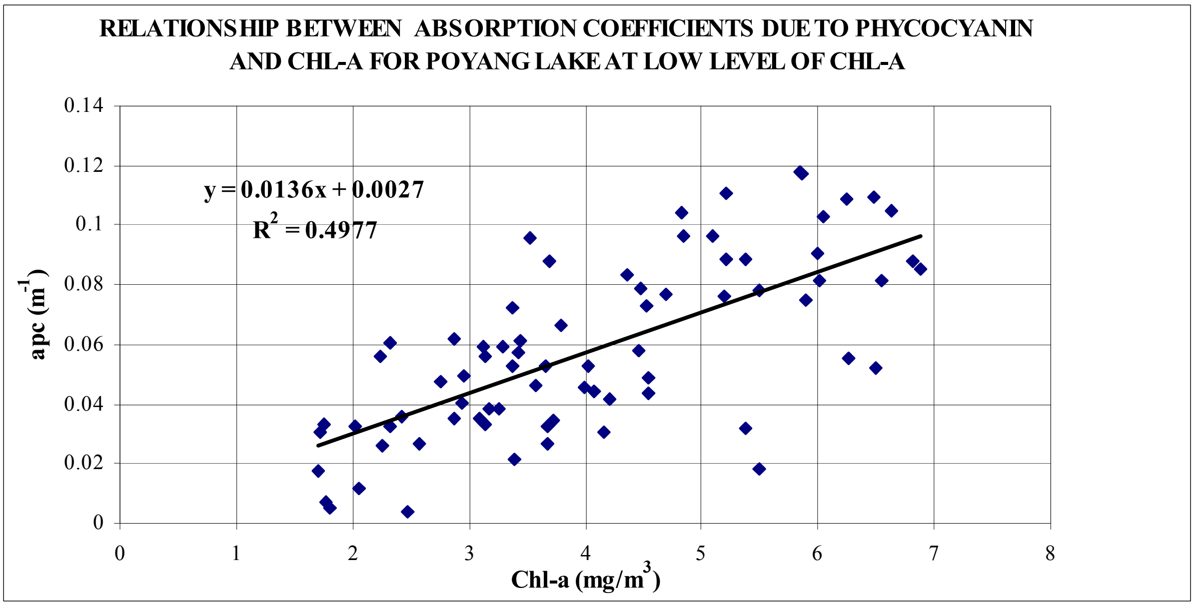

Figure 5.2-3: Relationship between Phycocyanin absorption coefficients and Chlorophyll a at low level of Chl-a

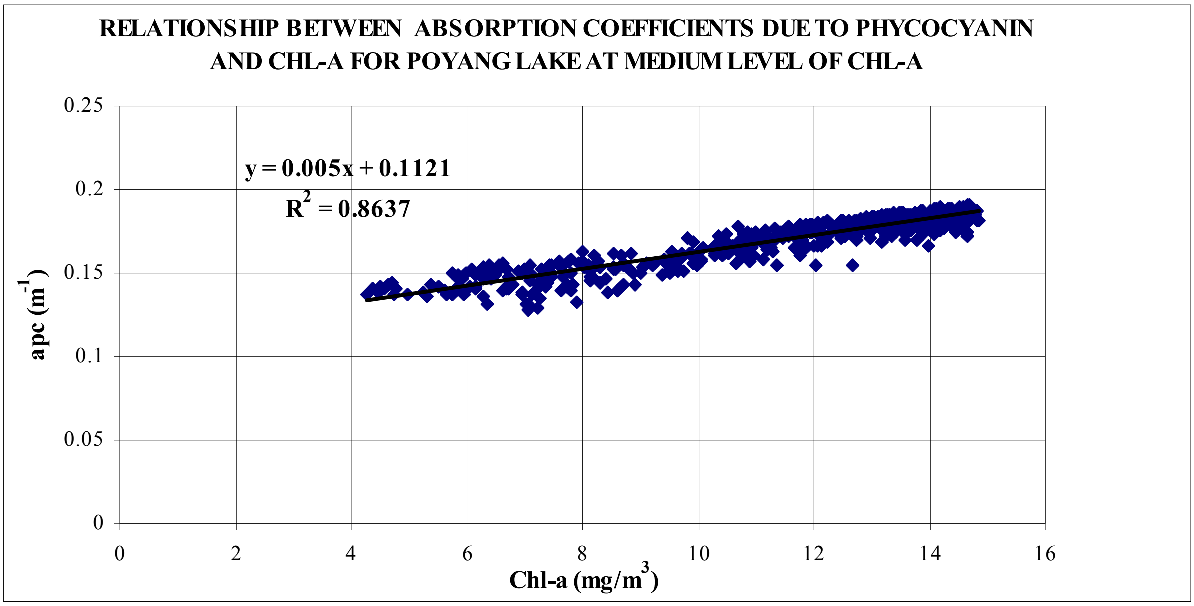

Figure 5.2-4: Relationship between Phycocyanin absorption coefficients and Chlorophyll a at medium level of Chl-a

5.3. Water quality parameters derived from Roxo reservoir

The derived analytical method was applied on the images on Roxo reservoir for two suitable images out of six. These images are dated 02-October-2006 and 29-May-2007, however due to small size of Roxo reservoir the derived water quality parameters could not be visualized and therefore only values were extracted for analysis. The following two tables (Table 5.3-1 and Table 5.3-2) show extracted values from their corresponding images:

Table 5.3-1: Derived water quality parameters for 02-10-2006 image

	Min	Max	Mean	Stdev
Chl-a (mg/m^3)	0.550	37.811	4.600	8.417
a_{dg} (m^{-1})	0.003	2.246	0.122	0.324
b_{bp} (m^{-1})	0.000	0.053	0.004	0.012
a_{pc} (m^{-1})	0.007	0.262	0.117	0.073

Table 5.3-2: Derived water quality parameters for 29-05-2007 image

	Min	Max	Mean	Stdev
Chl-a (mg/m^3)	1.639	27.464	11.268	6.913
a_{dg} (m^{-1})	0.084	1.392	0.568	0.337
b_{bp} (m^{-1})	0.000	0.103	0.029	0.028
a_{pc} (m^{-1})	0.003	0.264	0.159	0.059

5.3.1. Method testing using Roxo reservoir data

In-situ water quality measurements on the Roxo reservoir were taken from a single point at difference times and as it can be noted that there are only two useful images and hence made it practically impossible to validate. Therefore Roxo derived parameters where used again to check model reliability by evaluating the relationship between a_{pc} and $a_{chl\text{-}a}$ as shown in Figure 5.3-1 and Figure 5.3-2 below:

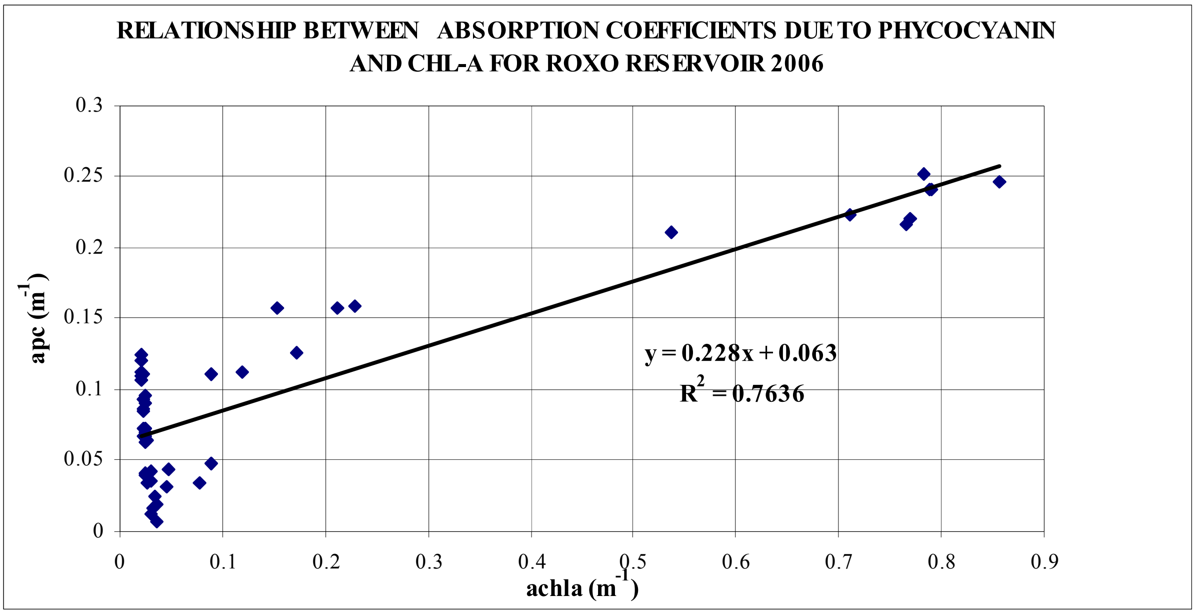

Figure 5.3-1: Relationship between Phycocyanin and Chlorophyll a absorption coefficients at Roxo-2006

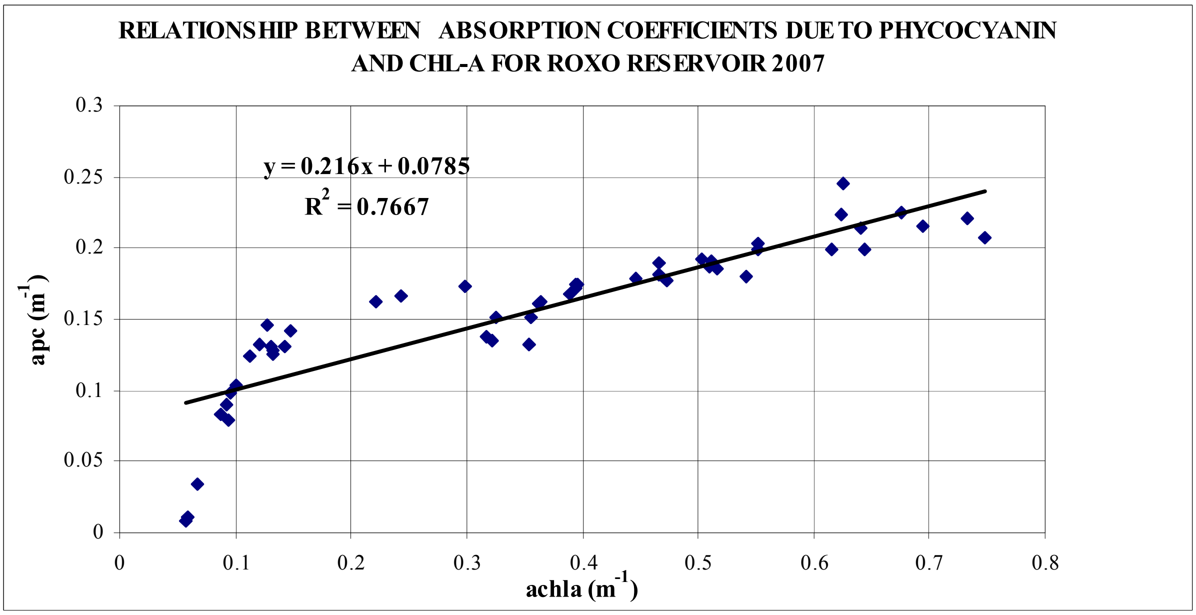

Figure 5.3-2: Relationship between Phycocyanin and Chlorophyll a absorption coefficients at Roxo-2007

5.3.2. Eutrophication Index derived from In-situ water quality measurements

The total of 25 in-situ water quality measurements were used to perform Principal Component Analysis (PCA) out of 32 because after visual inspections it was realized that some data were not given fixed values and they were unfit for analysis. Using PC analysis, coefficients of the first principal component for the five variables were extracted as shown in the Table 5.3-3 below:

Table 5.3-3: Coefficients of the first principal components for the five variables

Variables	Coefficient
Phosphate	0.365
Nitrates	0.098
Nitrites	0.381
Ammonia	0.509
Chlorophyll a	0.292

Therefore Eutrophication Index derived from In-situ measurements as per equation 4.1-1 will be as follows:

$$E.I = 0.365C_{PO4} + 0.098C_{NO3} + 0.381C_{NO2} + 0.509C_{NH3} + 0.292C_{chl-a} \qquad (5.3\text{-}1)$$

Using equation 5.3-1, eutrophication indices were calculated with respect to their corresponding in-situ water quality parameters (see appendix E) and summarized in Table 5.3-4 below:

Table 5.3-4: Summary of Eutrophication Indices derived from In-situ water quality measurements for Roxo reservoir

Year	Minimum	Maximum	Average	Stdv
2005	0.076	0.542	0.255	0.185
2006	0.035	0.356	0.173	0.127
2007	0.208	0.406	0.324	0.082

5.3.3. Eutrophication Index derived from Remote sensing data

Derived parameters are remote sensing products therefore; remote sensing eutrophication indices were calculated by applying principal component analysis on the derived parameters to generate coefficients of the first principal component which are summarized in the Table 5.3-5.

Table 5.3-5: Coefficients of the first principal components derived from the Images

Variables	Coefficient
Absorption coefficients due to Chlorophyll a pigments	0.539
Absorption coefficients due to Dissolved organic matter	0.511
Backscattering coefficients due	0.520

Variables	Coefficient
to Particulate matter	
Absorption coefficients due to Phycocyanin pigments	0.423

Using the above remote sensed derived principal component coefficients, remote sensed eutrophication index (R.S.E.I.) can be expressed as follows:

$$R.S.E.I = 0.539a_{chla} + 0.511a_{dg} + 0.520_{bp} + 0.423a_{pc} \qquad (5.3\text{-}2)$$

Applying equation 5.3-2 above on Inherent optic properties (IOPs) derived from the images as a result of applying proposed analytical method; R.S.E.I will be extracted for all available points (see appendices F and G) and are summarized on the **Error! Reference source not found.** below:

Table 5.3-6: Summarized Remote sensed eutrophication indices

Year	Minimum	Maximum	Average	Stdv
2006	0.029	0.929	0.185	0.265
2007	0.082	1.233	0.562	0.284

5.4. Demonstration results for large water bodies

For demonstration purposes and to get a clear picture on how derived products appear when the method is applied on large water bodies, available full resolution MERIS image of Bohai sea dated 14th February 2004 was used and the derived products are presented below (Figure 5.4-1, Figure 5.4-2, Figure 5.4-3, and Figure 5.4-4):

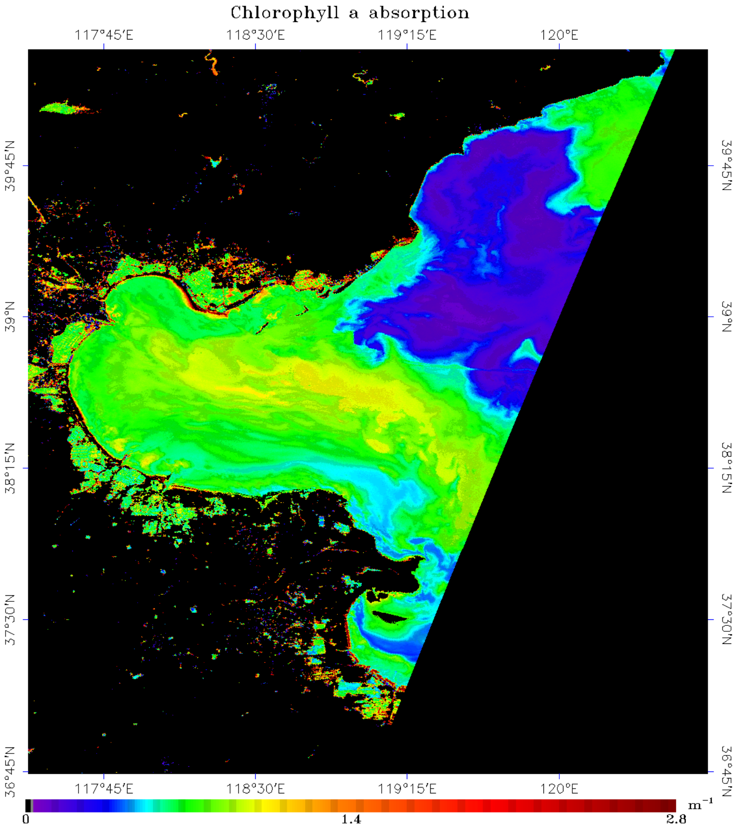
Chlorophyll a absorption

Figure 5.4-1: Derived Chlorophyll a absorption

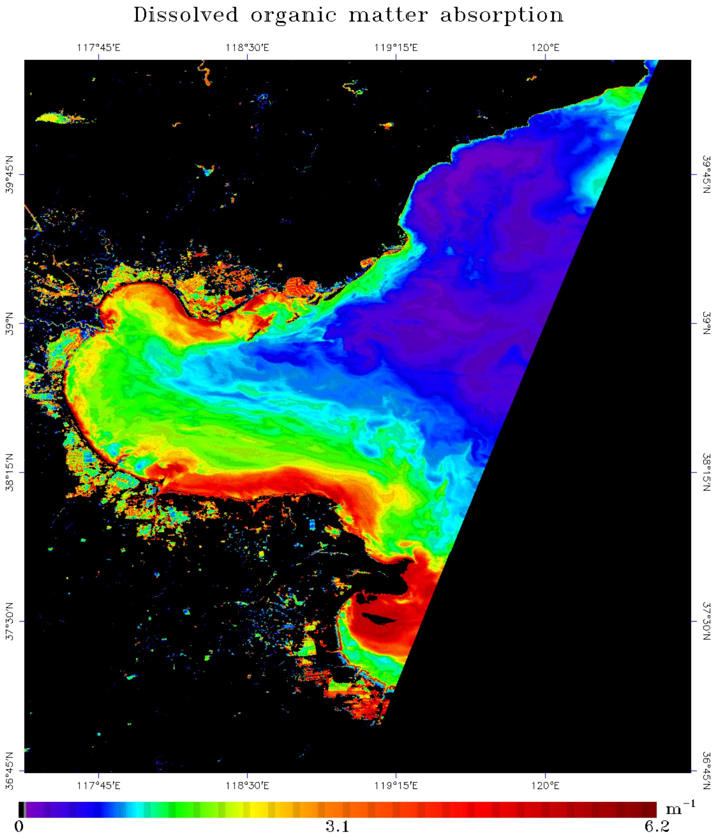
Dissolved organic matter absorption

Figure 5.4-2: Derived absorption coefficients due to dissolved organic matters

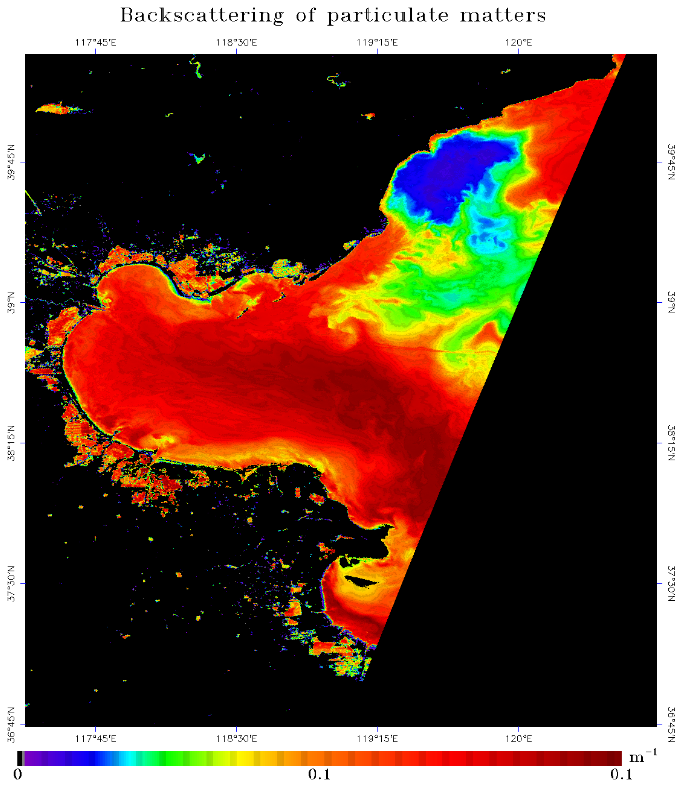

Figure 5.4-3: Derived backscattering coefficients due to particulate particles

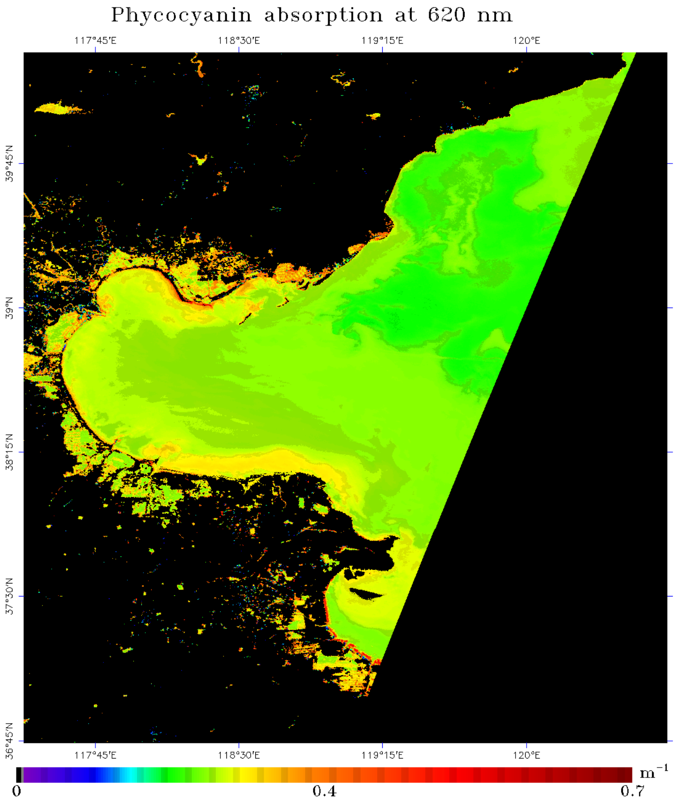

Figure 5.4-4: Derived absorption coefficients due to phycocyanin pigments

6. Discussion

6.1. Poyang lake

Developed analytical approach was applied on MERIS images of Poyang Lake and gave Chlorophyll a concentration, absorption coefficients due to dissolved organic matter, phycocyanin pigments and backscattering coefficients due to particulate particles as the final products. Derived Chlorophyll a concentration range from 0.06 to 30 mg/m^3; absorption coefficients due to dissolve organic matters range from 0.005 to 3.9 m^{-1}; backscattering coefficients due to particulate matters range from 0 to 0. 028 m^{-1} and absorption coefficients due phycocyanin pigments range from 0 to 0.39 m^{-1}. It can be noted that, proposed model gives higher values of Chlorophyll a concentration which goes up to 30 mg/m^3. In-situ water quality measurements were taken for three days (15th, 18th and 19th October 2008) but there was only one image which coincides with in-situ measurements which is the image for 19th October 2008. This coinciding image which is reduced resolution was used for validation; only six points were coinciding and gave higher relative errors for both Chlorophyll a and SPM. Relative errors were ranging from 18 to 33% and 9 to 32% for Chlorophyll a and SPM respectively.
This poor performance of proposed analytical model can be attributed by following factors:

- Error caused by MERIS instrument during image acquisition pile up in the derived parameters (Salama et al. 2009 b),
- Atmospheric correction applied is reasonable but not 100% accuracy which in turn contributing to the total error to the derived parameters,
- Full resolution of MERIS image has a spatial resolution of 300 m and reduced resolution has around 1000 m of which on retrieval the average value at the middle of the pixel is taken while in-situ measurements are done in scale of around 5 by 5 m area, therefore errors are introduced because of different spatial resolution,
- MERIS has 15 bands but only 12 bands used during processing and therefore reduced number of bands also reduce accuracy of retrieved parameters, and
- Though we have separated Chlorophyll a concentration with Phycocyanin pigments but still there is the possibility of having other Phytoplankton species with the overlapping spectral characters with Chlorophyll a which may cause over estimation of Chlorophyll a concentration derived from the images.

Validation of the model went further on the study of the relationship between two derived parameters; Chlorophyll a concentration and absorption coefficients due to Phycocyanin pigments. Derived absorption coefficients due Phycocyanin pigments were plotted against derived Chlorophyll a concentration using all points as a scatter plot (Figure 5.2-2) which do not give a clear trend, therefore the plot was clustered for further analysis and leads to more other two plots (Figure 5.2-3 and Figure 5.2-4). Clusters were identified based on the level of Chlorophyll a concentrations which are:

- Low Chlorophyll a concentration (0- 6 mg/m^3),
- Medium Chlorophyll a concentration (6- 15 mg/m^3), and
- High Chlorophyll a concentration (above 15 mg/m^3),

Coefficients of determination (R^2) are 0.5 and 0.86 for low and medium Chl-a concentration respectively. From the graphs, the following are observed:

- There is varying linear relationship between derived Chlorophyll a and a_{pc},
- Absorption coefficients due to phycocyanin pigment reaches maximum peak of around 0.221 m^{-1} when chlorophyll a concentration is between 15 and 20 mg/m^3, and
- Beyond the peak of phycocyanin absorption, it starts to decrease as Chl a concentration increases.

Linear relationship at low and medium concentration of Chl-a is one of the strength of the developed model because algae and cyanobacteria occurs together (Simis et al. 2007) so these two Phytoplankton species increase together at some points.

At the point where there is peak a_{pc} and a_{pc} decreases as Chlorophyll a increases can be explained by first referring to the characteristics of cyanobacteria. According to Schreurs, (1992) and Mur et al., (1993), cyanobacteria can be grouped into four groups according to their behaviour in water column as listed hereunder:

- Species able to fix nitrogen,
- Stratifying species which can regulate their buoyancy,
- Turbulent species which get well mixed in the epilimnion (this is the top layer in a thermally stratified lake or reservoir), and
- Colony or aggregate forming species.

With regard to above mentioned characteristics of cyanobacteria species, it is clear that as the water body become more eutrophic, nutrients, light and dissolved oxygen become scarce. At this critical condition, cyanobacteria become dominant and their toxic potential cause reduction of other phytoplankton species (Figueiredo et al. 2006). This explain why at some point where water body become more eutrophic cyanobacteria growth is higher than other species and reaches a peak of their growth, however this peak growth is not maintained for longer as it can be observed shortly the peak drop and cyanobacteria decreases as chlorophyll a increases. It has been observed that after reaching maximum growth, cyanobacteria population is terminated by viruses by the process called viral lysis (Simis et al. 2005 a) as well as other factors like programmed cell death (Berman-Frank et al. 2004) and therefore this explain the fall of cyanobacteria population after reaching maximum growth peak.

6.2. Roxo reservoir

There were only two images available to derive water quality parameters for Roxo reservoir dated 02nd October 2006 and 29th May 2007. Their derived parameters are summarized in Table 5.3-1 and Table 5.3-2. These images had some clouds therefore after atmospheric correction some pixels were removed and Roxo reservoir is relatively small (having surface area of 13.6 km^2 comparing with Poyang lake with surface area of 1158 up to 2500 km^2). Roxo reservoir has fingered structure which resulted into reduced available suitable pixels and there is a possibility of having more bottom reflectance effect. These derived products can not be properly visualized because of the small size of the reservoir. In spite of constraints mentioned above, still using proposed analytical model trophic state of Roxo reservoir can be classified as referred to Chapman (1996) as it is Mesotrophic having mean Chlorophyll a concentration of 4.6 mg/m^3 for the year 2006, and Eutrophic having mean Chlorophyll a concentration of 11.27 mg/m^3 which corresponds to Chapman (1996) range of eutrophic states (Table 2.1-1). Image of year 2007 which coincide with results of another research done on the same project area in 2007 (Gurung 2007) which classify Roxo reservoir to be eutrophic as well.

In-situ water quality measurements were taken from only one available sampling point which is located almost at the edge of the reservoir (see Figure 3.1-1). This location of sampling point was not covered in those two images and made it impossible to compare the results; however, as it can be observed from those two tables (Table 5.3-1 and Table 5.3-2) derived Chlorophyll a is higher than in-situ measured which is explained by the same facts as for Poyang Lake (6.1). Reliability of the derived model however, was assessed by studying relationship between derived a_{pc} and a_{chl-a} as can be referred on Figure 5.3-1 and Figure 5.3-2, the relation is linear ($R^2= 0.76$) for year 2006 and $R^2= 0.77$ for year 2007. As it can be noted also, the trend is the same as for Poyang data set that at low Chlorophyll a concentration the relation is non linear therefore these tests confirms model reliability.

Eutrophication indices were derived from Insitu measurements using Principal Component analysis as proposed by Parinet et al. (2004) and Primpas et al. (2009) see appendix E. Using the same concept of PCA, Remote sensed eutrophication indices using coefficients of absorptions and backscattering were derived (appendix F and G) and their statistics are presented on Table 5.3-4 and Table 5.3-6. Both in-situ and remote sensed indices have about the same average ranges, from 0.17 to 0.3 and from 0.19 to 0.56 respectively. A method to derive both (in-situ and remote sensed) eutrophication indices have been demonstrated and indices have been calculate for both in-situ and remote sensed data however based on the nature of these two data sets (In-situ and Remote sensed) is not possible to study their trend as was expected because in-situ eutrophication indices were derived from a single point while those from remote sensed data were derived from well distributed points all over the Reservoir. The derived R.S.E.I equation has positive coefficients for all derived IOPs which suggest that increase of these IOPs will lead to increase of eutrophication which is scientifically logical and make this model to be reliable.

7. Conclusions and Recommendations

7.1. Conclusions

The main objective of this research was to derive a remote sensing tool for monitoring and predicting eutrophication of inland waters which can surrogate existing inefficient in-situ measurement methods. Resulting from the research, the following are concluded:

- It has been observed that, it is not feasible to use remote sensing techniques (especially MERIS) with coarse spatial resolution for management of water quality of relatively small water bodies, a reference can be taken as 1000 km^2 as minimum surface area (as referred to Poyang Lake),
- Roxo reservoir is categorized as eutrophic water body based on the derived analytical model, which coincide with other researches regardless of its over estimation of Chlorophyll a concentrations and therefore proves its general usability,
- The relation between derived Chlorophyll a concentration and a_{pc} is strong (R^2 ranges from 0.5 to 0.9) which indicate that, derived analytical method may be reliable and can be used as a tool to derive indicators of eutrophication in large inland water bodies,
- The method shows that it is possible to separate harmful cyanobacteria from other phytoplankton species using remote sensing techniques which suggest that it is possible in future to deal with cyanobacteria only due to their raised concern in water quality management,
- It is possible to use derived analytical model to generate time series of eutrophication indicators for relatively large water bodies to study phytoplankton species changes over time and other changing parameters,
- There is a possibility of replacing in-situ derived eutrophication index with remote sensed eutrophication index for monitoring and predicting eutrophication in large inland water bodies, though its usability needs further investigations, and
- Performance of derived analytical model for Chlorophyll a concentration is poor because of over estimation of derived concentration, though its performance on a_{pc} was not tested because there was no available in-situ measurements,

7.2. Recommendations

- Around 620- 624 nm which is the target band for retrieval of phycocyanin pigment, there is a possibility of overlapping of absorption with other phytoplankton pigments, therefore this overlap has to be studied in details and understood so as to avoid errors during the retrieval of phycocyanin pigment,
- Phycocyanin pigments have to be considered in the normal routine water quality measurements because they are perfect indicators for cyanobacteria biomass which are of raising concern in water quality management,

- There should be a standard method to measure Phycocyanin pigment which will be used as a reference by scientific community as there is none in place at the moment as this will help to minimize errors in the whole process of measuring and comparing the measurements ,
- In-situ water quality sampling for validation must be evenly distributed all over the water body rather than be localized at only one point (as it has been observed for Roxo reservoir) so as to have a good representative data which will accommodate the spatial variability nature of water,
- Specific absorption coefficients for Chlorophyll a and Phycocyanin pigments are not constant for all water bodies all over the world so they have to be measured for each specific water body in order to have more accurate pigments concentrations derived from their absorption coefficients using Beer's Lambert law ,
- In-situ spectrometric measurements have to be taken for evaluation of atmospheric correction method and validation of derived water quality parameters parallel to water quality in-situ measurements,
- All in-situ measurements must strictly follow specifications as well as the standard calibration of instruments to minimize errors,
- Vast amount of in-situ water quality measurements is needed for derivation of actual E.I from PCA and further statistical analysis has to be performed to derive ranges of E.I with their corresponding eutrophic status,
- R.S.E.I derived from IOPs (a_{chla}, a_{dg}, bb_p and a_{pc}) have to be studied in depth to get a better understanding on how it can surrogate in-situ derived E.I,
- A better understanding of the threshold at which Chl-a increase linearly with Phycocyanin pigments is needed to be able to develop their relationship at that point,
- The two eutrophication indicators have to be well studied with respect to other factors which influence them and see the possibility of predicting one using another under specific conditions like temperature, nutrients levels and underwater light field, and
- As it is well know that SPM and CDOM do alter the amount of light getting into water bodies, therefore their effect should be studied in relation to Eutrophication and remote sensing.

References

Albert, A., et al. (2003). "An analytical model for subsurface irradiance and remote sensing reflectance in deep and shallow case- 2 waters." Optical Society of America **11**.

Alikas, K., et al. (2008). "Validation of the MERIS products on large European lakes: Peipsi, Vänern and Vättern." Hydrobiologia **599**(1): 161-168.

Berman-Frank, I., et al. (2004). "The demise of the marine cyanobacterium, *Trichodesmium* spp., via an autocatalyzed death pathway." Limnology and Oceanography **49**: 997- 1005.

Bezy, J. L., et al. (2000). "MERIS- A New Generation of Ocean- Colour Sensor onboard Envisat." eesa bulletin.

Bricaud, A., et al. (1981). "Absorption by dissolved organic-matter of the sea (yellow substance) in the UV and visible domains." Limnology and Oceanography **26**: 43- 53.

Bryant, D. A. (1994). "The molecule biology of cyanobacteria." Kluwer: Academic Publisher.

Bukata, R. P. (2005). Satellite Monitoring of Inland and Coastal Water Quality: Retrospection, Introspection, Future Directions. Ontario, CRC.

Carlson, R. E. (1977). "A trophic state index for lakes." Limnology and Oceanography **22**: 361- 369.

Chapman, D. (1996). Water Quality Assessments: A Guide to the use of Biota, Sediments and Water in Environmental Monitoring. London, Taylor and Francis.

Chorus, I., et al., Eds. (1999). Toxic Cyanobacteria in Water: A guide to their public health consequences, monitoring and management. London, WHO.

Dekker, A. G. (1993). Detection of optical water quality parameters for eutrophic waters by high resolution remote sensing. Amsterdam, Vrije University. **Phd**.

Doerffer, R., et al. (2007). The MERIS case 2 water algorithm, Taylor & Francis Ltd.

Doerffer, R., et al. (2008). MERIS Regional Coastal and Lake Case 2 Water Project Atmospheric Correction ATBD. Algorithm Theoretical Basic Document, GKSS GmbH.

Dokulil, M. T., et al. (2000). "Cyanobacterial dominance in lakes." Hydrobiologia **438**(1): 1-12.

Figueiredo, D. R. d., et al. (2006). "The effect of environmental parameters and cyanobacterial blooms on phytoplankton dynamics of a Portugal temperate lake." Hydrobiologia **568**: 145- 157.

Gamises, F. (2009). The study of spatial and temporal aspects of denitrification processes in Roxo catchment, Portugal. Water Resources. Enschede, ITC. **Masters**.

Giordani, G., et al. (2009). "Simple tools for assessing water quality and trophic status in transitional water ecosystems." Ecological Indicators **9**(5): 982-991.

Gons, H. J. (1999). "Optical teledetection of chlorophyll a in turbid inland waters." Environmental Science & Technology **33**(7): 1127-1132.

Gordon, H. (1976). "Radiative- transfer in ocean- method for determination of absorption and scattering properties." Applied optics **15**: 2611- 2613.

Gordon, H., et al. (1988a). "A semianalytical radiance model of ocean color." Journal of Geophysical Research **93**: 10,909- 910,924.

Gordon, H. R., et al. (1988b). "A Semianalytic Radiance Model of Ocean Color." Remote Sensing and Environment Optics.

Gurung, R. P. (2007). Modelling of Eutrophication in Roxo Reservoir, Alentejo, Portugal- A System Dynamic Based Approach. GEM. Enschede, ITC. **Master of Science:** 112.

Kagalou, I., et al. (2009). "Typology, classification and management issues of Greek lakes: implication of the Water Framework Directive (2000/60/EC)." Environmental Monitoring and Assessment **150**(1): 469-484.

Khan, F., et al. (2005). "Eutrophication: An ecological vision." The Botanical Review **71**(4): 449-482.

Kothari, C. R. (2004). Research Methodology- Methods & Techniques. Delhi, New Age International (P) Limited.

Lacouture, R. V., et al. (2006). "Phytoplankton Index of Biotic Integrity for Chesapeake Bay and its Tidal Tributaries." **29**.

Maritorena, S., et al. (2002). "Optimization of a semi analytical ocean color model for global-scale application." Optical Society of America: 2705- 2714.

Moncheva, S., et al. (2002). "Application of eutrophication indices for assessment of the Bulgarian Black Sea coastal ecosystem ecological quality." Water Science and Technology **46**: 10.

Mur, L. R., et al. (1993). How to control undesirable cyanobacterial dominance. 5th Int. Conf. Conservation and management of lakes, Stresa.

Paralta, E., et al. (2005). "Assessing and modelling hardrock aquifer recharge based on complementary methodologies- a case study in Gabbros of Beja aquifer system."

Parinet, B., et al. (2004). "Principal component analysis: an appropriate tool for water quality evaluation and management--application to a tropical lake system." Ecological Modelling **178**(3-4): 295-311.

Pascal, A. F. (2008). Spatio- temporal groundwater recharge assessment: a data- integration and modelling approach. Enschede, ITC. **MSc:** 57.

Pope, R., et al. (1997). "Absorption spectrum (380- 700 nm) of pure water. II. Integrated cavity measurements." Applied optics **36**: 8710- 8723.

Portielje, R., et al. (1999). "Relationships between eutrophication variables: from nutrient loading to transparency." Hydrobiologia: 375- 387.

Primpas, I., et al. (2009). "Principal component analysis: Development of a multivariate index for assessing eutrophication according to the European water framework directive." Ecological Indicators **In Press, Corrected Proof**.

Rencher, A. C. (2002). Methods of Multivariate Analysis, John Wiley and Sons, Inc.

Ruiz-Verdú, A., et al. (2008). "An evaluation of algorithms for the remote sensing of cyanobacterial biomass." Remote Sensing of Environment **112**(11): 3996-4008.

Salama, M. S., et al. (2009 b). "Error decomposition and estimation of inherent optical properties." Applied optics **48**(26): 4947-4962.

Schalles, J. F., et al. (2000). "Remote detection and seasonal patterns of phycocyanin, carotenoid and chlorophyll pigments in eutrophic waters." Archiv fur Hydrobiologie Special Issues Advances in Limnology **55**: 153- 168.

Schreurs, H. (1992). Cyanobacterial dominance. Relation to eutrophication and lake morphology, University of Amsterdam. **Doctoral:** 198.

Sen, P. K., et al. (2005). "Use of GIS and remote sensing in identifying recharge zones in an arid catchment: a case study of Roxo river basin, Portugal." Nepal geology society **31**(1): 25- 32.

Sheth, J. N. (1971). "The Multivariate Revolution in Marketing Research." Marketing **35**: 13- 19.

Simis, S. G. H., et al. (2005 b). "Remote Sensing of the Cyanobacterial Pigment Phycocyanin in Turbid Inland water." Limnology and Oceanography **50**: 237- 245.

Simis, S. G. H., et al. (2007). "Influence of phytoplankton pigment composition on remote sensing of cyanobacterial biomass." Remote Sensing of Environment **106**(4): 414-427.

Simis, S. G. H., et al. (2005 a). "Optical changes associated with cyanobacterial bloom termination by viral lysis." Plankton research **27**: 937- 949.

Smith, R., et al. (1981). "Optical properties of the clearest natural waters (200- 800 nm)." Applied optics **20**: 177- 184.

Tusseau-Vuillemin, M. H. (2001). Do food processing industries contribute to the eutrophication of aquatic systems?

Vithanage, I. C. B. (2009). Analysis of Nutrient Dynamics in Roxo Catchment Using Remote Sensing Data and Numerical Modelling. WRS. Enschede, ITC. **MSc**.

Xichang, Z. (2009). Characterization of the Specific Inherent Optical Properties of the Poyang Lake and Quantification of Water Turbidity Using Remote Sensing and a Semi- Analytical Bio- Optical Inversion Model for Shallow Waters. Water Resources Enschede, ITC. **Masters:** 53.

Yang, D., et al. (2006). "Hyperspectral retrieval model of phycocyanin in case II waters." Chinese Science Bulletin **51**(0): 149-153.

Appendices

Appendix A: Meteorological data from Aljustrel station- Portugal (2005- 2008)

Average Minimum monthly temperature (^{0}c)

	2005	2006	2007	2008
January	-0.2290	3.0168	3.3032	5.8013
February	-0.2905	4.0371	7.0225	7.3628
March	6.7200	7.2052	5.3400	6.0600
April	6.8700	9.1867	8.2737	8.7890
May	11.1865	10.6516	10.4323	10.2919
June	15.2100	14.2567	13.2300	13.1300
July	15.2806	16.0452	14.4806	15.1032
August	16.0355	16.1065	14.7516	14.6819
September	12.8367	15.1567	15.0967	14.0217
October	13.1065	14.1048	10.9555	10.3668
November	6.9787	11.5567	4.9453	3.8523
December	5.3429	3.7333	3.7806	4.4842

Average Maximum monthly temperature (^{0}c)

	2005	2006	2007	2008
January	16.6581	14.7568	16.0387	17.6758
February	17.1476	15.9629	17.7989	18.7655
March	21.5067	19.1297	19.8926	19.5590
April	24.4667	23.1733	21.6960	22.5790
May	28.0697	28.6000	25.3387	22.6484
June	32.9700	31.1133	28.4900	31.3033
July	33.7742	34.8484	33.7161	31.8516
August	35.6968	35.7581	32.8871	32.0852
September	31.7667	31.7300	30.2333	28.9117
October	25.6806	26.1510	26.2297	24.4755
November	18.3143	21.5900	21.6653	18.8973
December	16.0542	16.3367	16.4387	14.8906

Average monthly precipitation (mm)

	2005	2006	2007	2008
January	0.0290	1.4516	0.9742	2.5355
February	0.1286	1.3179	1.6036	3.1655
March	0.4067	3.0355	0.4581	0.9516
April	0.1200	1.4667	2.8133	2.7467
May	1.6839	0.0097	1.9548	1.4194
June	0.0033	0.4033	0.8033	0.0033
July	0.0839	0.0806	0.0097	0.0000
August	0.0065	0.2097	0.4000	0.0161
September	0.0733	0.6133	0.8533	1.2367
October	4.1161	5.6258	0.4774	1.2419
November	2.7200	10.2633	1.3443	1.2633

	2005	2006	2007	2008
December	2.1065	1.6500	0.8677	1.8968

Appendix B: In-situ water quality measurements for Roxo reservoir (2005-2008)

Recorded Date	Phosphates	Nitrates	Nitrites	Ammonia unionized	Chlorophyll-a
11-01-2005	0.023	5.090	0.027	0.012	0.060
09-02-2005	0.034	0.930	0.032	0.021	0.045
08-03-2005	0.121	1.240	0.037	0.083	0.015
05-04-2005	0.042	1.280	0.034	0.016	0.009
31-05-2005	0.036	2.390	0.001	0.008	0.014
26-07-2005	0.026	0.590	0.003	0.004	0.019
06-09-2005	0.023	0.630	0.010	0.038	0.029
29-11-2005	0.061	3.010	0.065	0.352	0.056
10-01-2006	0.037	3.190	0.072	0.001	0.007
07-02-2006	0.023	3.190	0.001	0.003	0.010
07-03-2006	0.025	2.970	0.003	0.020	0.009
04-04-2006	0.029	0.970	0.034	0.017	0.020
02-05-2006	0.027	1.020	0.011	0.026	0.011
30-05-2006	0.023	0.040	0.002	0.043	0.009
26-06-2006	0.045	1.200	0.001	0.023	0.044
26-07-2006	0.040	0.090	0.001	0.012	0.019
05-09-2006	0.059	0.130	0.001	0.021	0.034
02-10-2006	0.115	0.090	0.003	0.005	0.012
28-11-2006	0.113	2.000	0.155	0.010	0.002
02-01-2007	0.050	3.800	0.020	0.011	0.007
30-01-2007	0.035	3.100	0.062	0.007	0.004
27-02-2007	0.023	3.200	0.054	0.005	0.011
27-03-2007	0.033	2.000	0.065	0.007	0.008
02-05-2007	0.023	2.000	0.080	0.030	0.003
29-05-2007	0.023	2.000	0.012	0.001	0.048
25-06-2007	0.023	2.000	0.008	0.002	0.013
23-07-2007	0.023	2.000	0.003	0.000	0.006
11-09-2007	0.023	2.000	0.004	0.002	0.019
01-10-2007	0.023	3.900	0.002	0.001	0.018
29-10-2007	0.023	2.000	0.019	0.003	0.004
27-11-2007	0.023	2.000	0.123	0.001	0.003
02-01-2008	0.023	2.000	0.072	0.010	0.002

All measurements are in mg/l

Appendix C: Atmospheric correction of MERIS images

Open source tool box for analysis and processing EO data (BEAM) was used to perform atmospheric correction on the MERIS images, the tool has plug in called Case 2 Regional Processor (c2r) which is used to perform atmospheric correction using the algorithm described in the Algorithm Theoretical Basic Document (ATBD) (Doerffer et al. 2008). The procedures followed for atmospheric correction in BEAM are summarized in the figure below (Doerffer et al. 2008):

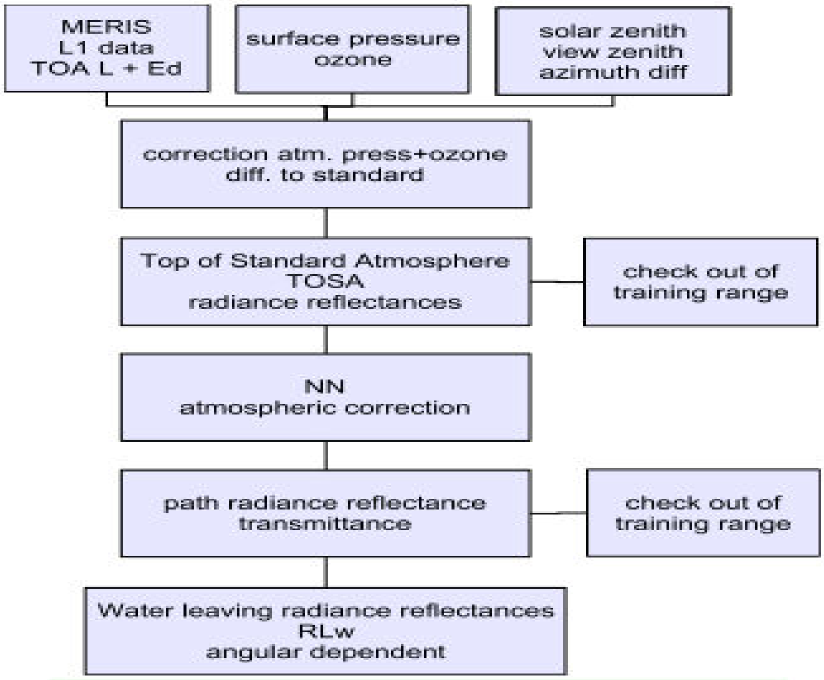

Flow of Atmospheric correction procedure

There are 4 bands in MERIS used for atmospheric correction (band 9, 10, 12 and 13), however, to avoid errors due to extrapolation of the results from four bands into the blue- green spectral range, 12 out of 15 MERIS bands have been used for AC (excluding band 11, 14 and 15). In the process of atmospheric correction, neural network is used to establish relationship between radiance reflectance at the top of standard atmosphere (TOSA) and water leaving radiance reflectance for all 12 used bands, and the process is summarized in the figure below (Doerffer et al. 2008):

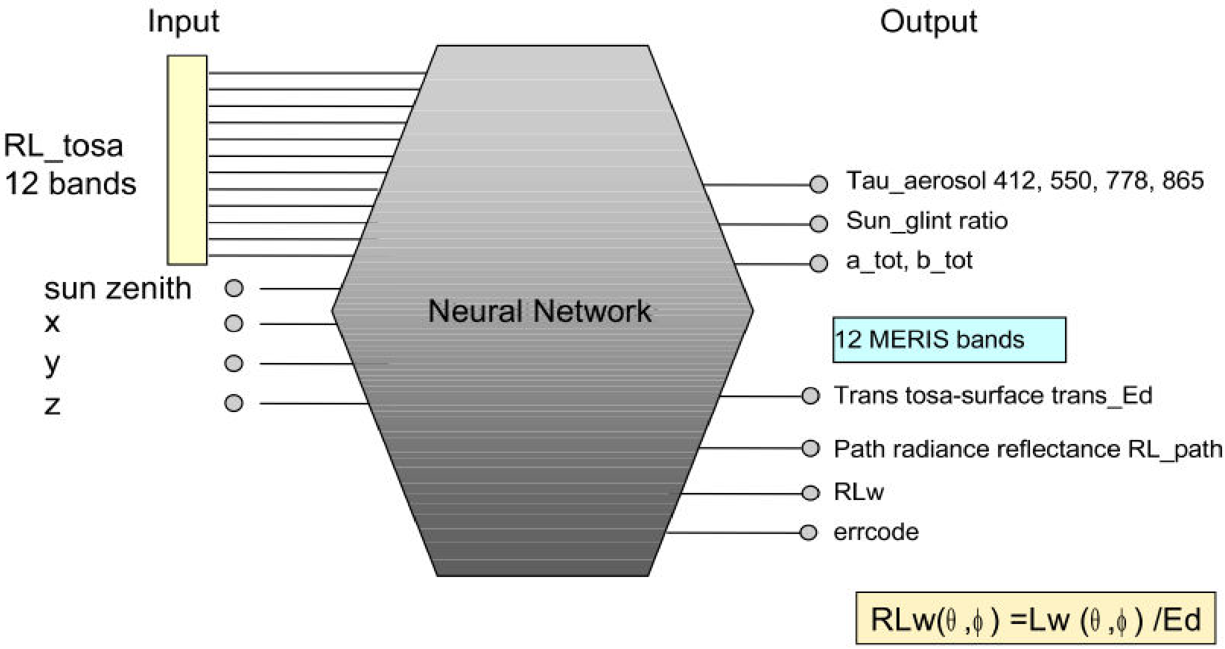

Outline of the neural network to determine the water leaving radiance reflectance (RLw)

The accuracy of the method was checked using in-situ from Poyang lake in China which gave good correlation with R^2 ranging from 0.8722 to 0.9342 (see main document). Therefore AC was performed straight using BEAM VISAT C2R plug as summarized above and the resulting water leaving radiance reflectance [RLw(sr^{-1})] for 12 (1- 10, 12 and 13) bands were used for further processing.

Appendix D: Retrieval of PC concentration using Simis model

Phycocyanin absorption coefficient was first determined based on (Simis et al. 2005 b) model, the model consider chlorophyll a and phycocyanin pigments are the major light absorbers water constituents. The concept of band ratios was used based on the spectral reflectance relationship (Gordon et al., 1975) and empirical coefficients. The implementation of band ratios took into consideration that Chlorophyll a has maximum absorption at 665 nm (Dekker 1993; Gons et al., 2002b) and Phycocyanin pigments have maximum absorption at 620 nm (Bryant 1994). Two ratios have been used to retrieve a_{pc}; ratio one uses reflectance (R) at 709 nm (λ2) and 665 nm (λ1) to retrieve chl a, and ratio two uses reflectance at 709 nm (λ2) and 620 nm (λ1) to retrieve a_{pc} and the two ratios equations were solved simultaneously as follows:

- Relation by Gordon et al. (1975) which relate IOPs and AOPs was implemented:

$$R\left(0^-,\lambda\right)=f\frac{b_b(\lambda)}{a(\lambda)+b_b(\lambda)} \tag{1}$$

Since f and b_b are spectrally neutral, then symbol λ can be ignored in front of b_b, by applying reflectance ratios [R (λ_2): R (λ_1)] will give the following relation:

$$\frac{R(\lambda_2)}{R(\lambda_1)}=\frac{a(\lambda_1)+b_b}{a(\lambda_2)+b_b} \tag{2}$$

- The absorption by water and its constituents at wavelength $\lambda_1[a(\lambda_1)]$ is solved from equation 2, as follows:

$$a(\lambda_1)=\frac{R(\lambda_2)\times(a(\lambda_2)+b_b)}{R(\lambda_1)}-b_b \tag{3}$$

- Ratio 1 (λ_2= 709 and λ_1= 665 nm) is used to retrieve the absorption by Chl-a in eutrophic inland water, while ratio 2 (λ_2= 709 and λ_1= 620 nm) is used to retrieve the PC absorption,
- Simplification is made by neglecting pigment absorption at 709 nm and absorption by CDOM and tripton is considered negligible and instead introducing empirical coefficient as a correction factor γ (Simis et al. 2005 b) to get the following equation (from R1 relation):

$$a_{chl}(665)=\left[\frac{R(709)\times(a_W(709)+b_b)}{R(665)}-b_b-a_W(665)\right]\times\gamma^{-1} \tag{4}$$

- b_b is retrieved from 778.75 nm, 15 nm wide band (Gons 1999) by solving eq. 1 for $a(778.75)= a_W(778.75)$ and a value for f that is realistic for turbid waters,

$$R(778.75)=f\frac{b_b}{a_w(778.75)+b_b} \tag{5}$$

$$b_b=\frac{R(778.75)\times a_w(778.75)}{f-R(778.75)} \tag{6}$$

- ratio 2 is using 620 nm as λ_1 which correspond to reflectance due to cyanobacteria rich waters; re writing eq. 4 for band ratio 2 and introducing correction factor δ for the correction of $a(620)$ to get:

$$a_{chl}(620) + a_{pc}(620) = \left[\frac{R(709) \times (a_W(709) + b_b)}{R(620)} - b_b - a_W(620) \right] \times \delta^{-1} \tag{7}$$

- To relate $a_{chl}(665)$ to $a_{chl}(620)$ the conversion factor ε is introduced to obtain:

$$a_{pc}(620) = \left[\frac{R(709) \times (a_W(709) + b_b)}{R(620)} - b_b - a_W(620) \right] \times \delta^{-1} - \left[\varepsilon \times a_{chl}(665) \right] \tag{8}$$

Finally [PC] was derived using specific absorption coefficient of PC [$a^*_{pc}(620)$] of 0.0095 m^2/mg PC from the following relation below:

$$[PC] = \frac{a_{pc}(620)}{a^*_{pc}(620)} \tag{9}$$

From the experiments (Simis et al. 2005 b) the following values for correction and conversion factors were obtained:

- $\gamma = 0.68$,
- $\delta = 0.84$, and
- $\varepsilon = 0.24$

Introduced correction factors γ and δ was retrieved from $R(0^-, \lambda)$ and $a(\lambda)_{ph}$ datasets, and conversion factor ε was iteratively retrieved from the best fit of computed versus observed PC concentration (Simis et al. 2005 b).

The proposed model is empirical and is therefore valid for the used data set only. For example applying Simis model to the Roxo MERIS images gave negative values for PC concentration and a_{pc}.

Appendix E: Eutrophication Index derived from In-situ water quality measurements for Roxo reservoir

Date	Phosphate	Nitrates	Nitrites	Ammonia	Chl-a	E.I
11-01-2005	0.023	5.090	0.027	0.012	0.060	0.54
09-02-2005	0.034	0.930	0.032	0.021	0.045	0.14
08-03-2005	0.121	1.240	0.037	0.083	0.015	0.23
05-04-2005	0.042	1.280	0.034	0.016	0.009	0.16
31-05-2005	0.036	2.390	0.001	0.008	0.014	0.26
26-07-2005	0.026	0.590	0.003	0.004	0.019	0.08
06-09-2005	0.023	0.630	0.010	0.038	0.029	0.10
29-11-2005	0.061	3.010	0.065	0.352	0.056	0.54
10-01-2006	0.037	3.190	0.072	0.001	0.007	0.36
07-02-2006	0.023	3.190	0.001	0.003	0.010	0.33
07-03-2006	0.025	2.970	0.003	0.020	0.009	0.31
04-04-2006	0.029	0.970	0.034	0.017	0.020	0.13
02-05-2006	0.027	1.020	0.011	0.026	0.011	0.13
30-05-2006	0.023	0.040	0.002	0.043	0.009	0.04
26-06-2006	0.045	1.200	0.001	0.023	0.044	0.16
26-07-2006	0.040	0.090	0.001	0.012	0.019	0.04
05-09-2006	0.059	0.130	0.001	0.021	0.034	0.06
02-10-2006	0.115	0.090	0.003	0.005	0.012	0.06
28-11-2006	0.113	2.000	0.155	0.010	0.002	0.30
02-01-2007	0.050	3.800	0.020	0.011	0.007	0.41
30-01-2007	0.035	3.100	0.062	0.007	0.004	0.35
27-02-2007	0.023	3.200	0.054	0.005	0.011	0.35
27-03-2007	0.033	2.000	0.065	0.007	0.008	0.24
23-07-2007	0.023	2.000	0.003	0.000	0.006	0.21
01-10-2007	0.023	3.900	0.002	0.001	0.018	0.40

Appendix F: Remote sensed eutrophication indices for 2006

Point	Lat (deg.)	Lon (deg.)	a_{chla} (m^{-1})	a_{cdom} (m^{-1})	b_{bp} (m^{-1})	a_{pc} (m^{-1})	R.S.E.I
1	37.946746	-8.038885	0.0308	0.0137	0.0001	0.0126	0.029
2	37.946746	-8.061329	0.0239	0.0103	0.0002	0.0692	0.047
3	37.94354	-8.045298	0.2117	0.3558	0.0019	0.1570	0.363
4	37.94354	-8.035679	0.0891	0.0446	0.0005	0.0476	0.091
5	37.94354	-8.061329	0.0212	0.0077	0.0003	0.1201	0.066
6	37.94354	-8.048504	0.0461	0.0197	0.0002	0.0318	0.048
7	37.94354	-8.070948	0.0214	0.0078	0.0003	0.1095	0.062
8	37.94354	-8.051711	0.0247	0.0094	0.0002	0.0731	0.049
9	37.94354	-8.038885	0.0890	0.0445	0.0005	0.0476	0.091
10	37.94354	-8.054917	0.0247	0.0094	0.0002	0.0729	0.049
11	37.940333	-8.064536	0.7832	0.4499	0.0081	0.2526	0.763

Point	Lat (deg.)	Lon (deg.)	a_{chla} (m^{-1})	a_{cdom} (m^{-1})	b_{bp} (m^{-1})	a_{pc} (m^{-1})	R.S.E.I
12	37.940333	-8.061329	0.0294	0.0123	0.0001	0.0423	0.040
13	37.940333	-8.058123	0.0225	0.0074	0.0001	0.0730	0.047
14	37.940333	-8.067742	0.0298	0.0138	0.0002	0.0356	0.038
15	37.940333	-8.074154	0.0205	0.0070	0.0003	0.1249	0.068
16	37.940333	-8.042092	0.0238	0.0098	0.0002	0.0628	0.044
17	37.940333	-8.054917	0.0255	0.0104	0.0001	0.0405	0.036
18	37.940333	-8.051711	0.0255	0.0104	0.0001	0.0404	0.036
19	37.940333	-8.070948	0.7104	0.4678	0.0286	0.2231	0.731
20	37.937127	-8.074154	0.0242	0.0100	0.0002	0.0676	0.047
21	37.937127	-8.061329	0.1533	0.1476	0.0011	0.1573	0.225
22	37.937127	-8.067742	0.0885	0.0444	0.0006	0.1106	0.117
23	37.937127	-8.070948	0.0885	0.0444	0.0006	0.1105	0.117
24	37.937127	-8.064536	0.7649	0.7777	0.0530	0.2159	0.928
25	37.933921	-8.070948	0.0240	0.0085	0.0003	0.0957	0.058
26	37.933921	-8.077361	0.8561	0.4551	0.0254	0.2459	0.811
27	37.933921	-8.074154	0.7687	0.7756	0.0485	0.2208	0.929
28	37.930714	-8.080567	0.0242	0.0090	0.0003	0.0904	0.056
29	37.930714	-8.067742	0.5372	0.2844	0.0065	0.2110	0.527
30	37.930714	-8.061329	0.0217	0.0053	0.0002	0.1071	0.060
31	37.930714	-8.070948	0.7894	0.3399	0.0188	0.2413	0.710
32	37.930714	-8.054917	0.0219	0.0063	0.0002	0.0927	0.054
33	37.930714	-8.058123	0.0219	0.0063	0.0002	0.0927	0.054
34	37.930714	-8.077361	0.0475	0.0171	0.0002	0.0440	0.053
35	37.930714	-8.064536	0.0224	0.0076	0.0003	0.1110	0.063
36	37.930714	-8.074154	0.7888	0.3394	0.0187	0.2412	0.710
37	37.927508	-8.061329	0.2285	0.2485	0.0019	0.1583	0.318
38	37.927508	-8.064536	0.0266	0.0100	0.0002	0.0644	0.047
39	37.927508	-8.070948	0.0358	0.0153	0.0001	0.0194	0.035
40	37.927508	-8.067742	0.0276	0.0113	0.0001	0.0405	0.038
41	37.927508	-8.051711	0.0217	0.0052	0.0002	0.1119	0.062
42	37.924302	-8.064536	0.1196	0.0543	0.0008	0.1120	0.140
43	37.921096	-8.058123	0.0224	0.0083	0.0002	0.0856	0.053
44	37.921096	-8.061329	0.0224	0.0083	0.0002	0.0857	0.053
45	37.921096	-8.064536	0.0344	0.0141	0.0001	0.0250	0.036
46	37.917889	-8.061329	0.0273	0.0116	0.0001	0.0342	0.035
47	37.914683	-8.058123	0.0227	0.0086	0.0002	0.0676	0.045
48	37.911477	-8.058123	0.0313	0.0143	0.0001	0.0171	0.031
49	37.908271	-8.061329	0.0767	0.0400	0.0004	0.0349	0.077
50	37.908271	-8.058123	0.1721	0.1369	0.0012	0.1259	0.216
51	37.905064	-8.054917	0.0357	0.0166	0.0001	0.0066	0.031

Appendix G: Remote sensed eutrophication indices for 2007

Point	Lat (deg.)	Lon (deg.)	a_{chla} (m^{-1})	a_{cdom} (m^{-1})	b_{bp} (m^{-1})	a_{pc} (m^{-1})	R.S.E.I
1	37.94811	-8.045	0.0915	0.1932	0.0008	0.0904	0.187
2	37.94811	-8.054	0.1328	0.3625	0.0012	0.125	0.310
3	37.94491	-8.064	0.1201	0.2392	0.0011	0.1328	0.244
4	37.94491	-8.073	0.6433	1.1087	0.0578	0.199	1.027
5	37.94491	-8.045	0.3537	1.0485	0.1032	0.1326	0.836
6	37.94491	-8.057	0.3215	0.9895	0.0927	0.135	0.784
7	37.94491	-8.077	0.1314	0.292	0.0013	0.1307	0.276
8	37.94491	-8.048	0.6254	0.4736	0.0097	0.2461	0.688
9	37.94491	-8.061	0.5098	0.7934	0.0478	0.1866	0.784
10	37.94491	-8.054	0.2214	0.4429	0.0021	0.1626	0.415
11	37.9417	-8.073	0.4668	0.7426	0.0489	0.181	0.733
12	37.9417	-8.077	0.0949	0.2018	0.0007	0.0981	0.196
13	37.9417	-8.038	0.5422	1.1837	0.0722	0.1806	1.011
14	37.9417	-8.048	0.0944	0.138	0.001	0.0794	0.155
15	37.9417	-8.051	0.6413	0.6958	0.0348	0.2137	0.809
16	37.9417	-8.07	0.6937	0.69	0.0334	0.2155	0.834
17	37.9417	-8.061	0.3163	0.9506	0.0867	0.1374	0.759
18	37.9417	-8.067	0.3883	0.776	0.0524	0.1675	0.704
19	37.9417	-8.064	0.615	0.8495	0.0454	0.1989	0.873
20	37.9417	-8.057	0.3548	0.9343	0.0732	0.1515	0.770
21	37.9385	-8.064	0.3254	0.8538	0.0664	0.1511	0.710
22	37.9385	-8.067	0.3631	0.8246	0.0587	0.1607	0.715
23	37.9385	-8.061	0.4724	0.8732	0.0556	0.177	0.804
24	37.9385	-8.07	0.5516	0.4125	0.0208	0.2026	0.604
25	37.9353	-8.07	0.3633	0.8007	0.0559	0.1622	0.702
26	37.9353	-8.061	0.1006	0.2188	0.0008	0.1041	0.210
27	37.9353	-8.077	0.5519	0.5319	0.0301	0.1987	0.669
28	37.9353	-8.067	0.4461	0.7392	0.0471	0.1781	0.718
29	37.9353	-8.073	0.0869	0.0843	0.0006	0.083	0.125
30	37.9353	-8.064	0.6232	0.4211	0.0135	0.2235	0.652
31	37.9353	-8.08	0.1322	0.3418	0.0012	0.1278	0.300
32	37.9321	-8.048	0.1433	0.4322	0.0014	0.1308	0.354
33	37.9321	-8.077	0.3937	0.6459	0.0422	0.1748	0.638
34	37.9321	-8.073	0.4661	0.3326	0.0204	0.1902	0.512
35	37.9321	-8.08	0.7326	0.5051	0.0213	0.2215	0.757
36	37.92889	-8.073	0.3933	0.7027	0.045	0.1725	0.667
37	37.92889	-8.077	0.3966	0.6594	0.0414	0.175	0.646
38	37.92889	-8.08	0.5039	0.5725	0.0333	0.1917	0.662
39	37.92889	-8.083	0.1268	0.2077	0.0011	0.1465	0.237
40	37.92569	-8.077	0.1119	0.1433	0.0008	0.1235	0.186
41	37.92569	-8.07	0.147	0.3162	0.0014	0.1425	0.302
42	37.92569	-8.073	0.2988	0.3042	0.0039	0.1732	0.392
43	37.92569	-8.067	0.5116	0.6294	0.0374	0.1915	0.697

Point	Lat (deg.)	Lon (deg.)	a_{chla} (m^{-1})	a_{cdom} (m^{-1})	b_{bp} (m^{-1})	a_{pc} (m^{-1})	R.S.E.I
44	37.92569	-8.064	0.5163	0.8763	0.0521	0.1848	0.831
45	37.92249	-8.067	0.6757	0.4744	0.0183	0.225	0.711
46	37.91929	-8.067	0.2427	0.3511	0.0026	0.1658	0.381
47	37.91608	-8.067	0.0575	0.0923	0.0003	0.0088	0.082
48	37.91608	-8.064	0.0675	0.0966	0.0004	0.0339	0.100
49	37.90968	-8.061	0.7481	1.3916	0.0604	0.2079	1.233
50	37.90648	-8.061	0.0584	0.1086	0.0003	0.0111	0.092